Towards a tracking of bird migratory behaviour through geological time: an isotopic and histological approach

Anaïs Duhamel[1,*], Aurore Canoville[2,3], Arnaud Vinçon-Laugier[1], Julien Joseph[4], François Fourel[4], Christophe Lécuyer[1], Romain Amiot[1,$] and Antoine Louchart[1,$]

[1] Univ Lyon, Univ Lyon 1, ENSL, CNRS, LGL-TPE, Villeurbanne, France
[2] Museum für Naturkunde, Leibniz-Institut für Evolutions- und Biodiversitätsforschung, 10115 Berlin, Germany
[3] North Carolina Museum of Natural Sciences, 27601 Raleigh NC, USA
[4] Université Claude Bernard Lyon 1, LEHNA UMR 5023, CNRS, ENTPE, F-69622 Villeurbanne, France
[*] Corresponding author, anais.duhamel@ens-lyon.fr
[$] Co-senior authors

Abstract

1. Bird seasonal migration is a remarkable biogeographic phenomenon, yet its deep-time origin(s) and evolutionary history remain poorly understood, with the bird fossil record largely overlooked. This study explores the predictability of bird migratory behaviour from the oxygen isotope composition of their bone apatite phosphate ($\delta^{18}O_p$), a promising approach in this regard because: (i) sedentary and migratory birds tend to occupy distinct climatic niches year-round; (ii) their $\delta^{18}O_p$ values primarily reflect the climate-driven isotopic composition of their drinking water; and (iii) this isotopic signature can persist through fossilisation.

2. Bone tissues were categorised based on their potential to yield spatio-temporally distinct climatic records: "early bone tissues" (EBT), deposited before somatic maturity, and "late bone tissues" (LBT), resulting from bone remodelling events over the lifespan. The predictability of migratory behaviour was theoretically assessed by modelling tissue-specific $\delta^{18}O_p$ values for thousands of birds across 77 migratory and sedentary species, based on their tracking or observational data, using a revised phosphate-water fractionation equation. These theoretical results were confronted with data from 11 extant bird species obtained using a new experimental framework that combines histological and isotopic analyses.

3. We emphasised that, under specific sampling protocols, a significantly positive correlation between the $\delta^{18}O_p$ value and the proportion of LBT of bone samples is characteristic of long-distance migratory birds. Additionally, migratory birds that perished outside their natal sites can be identified when their $\delta^{18}O_{p,EBT}$ value falls outside the range observed in local juvenile and sedentary birds.

4. We conclude that the migratory behaviour of birds can be inferred from the $\delta^{18}O_p$ values of their skeletal remains, with relatively low sensitivity (not all migratory behaviours are detected), but with high specificity (sedentary birds are rarely misclassified as migratory). We argue that the same method can be used to infer past bird migratory behaviours from well-preserved fossil bones, provided the palaeoclimatic context is carefully considered. More broadly, this study establishes a framework for inferring the migratory behaviour of any vertebrate from non-fully remodelled biomineralised remains.

Keywords: Bone tissues, Bird migration, Fossil birds, Fractionation equation, Oxygen isotopes, Stable isotopes.

1 INTRODUCTION

The evolution of birds has been profoundly shaped by the emergence of one of the most extensive biogeographic phenomena observed among vertebrates: seasonal migrations. Today, billions of birds, accounting for 20% of the avian species (Somveille, 2016), migrate twice a year between their breeding and wintering grounds, sometimes covering several thousand kilometres. This behaviour is thought to have evolved as an adaptive response to seasonally fluctuating environmental pressures, driven by a complex interplay between abiotic factors (e.g., climate seasonality) and biotic factors (e.g., competition for land and resources, predation and pathogens; Alerstam et al., 2003; Salewski & Bruderer, 2007). However, the deep-time origins and evolutionary history of avian migration – particularly in response to past climate changes (Louchart, 2008) – remain poorly understood. This knowledge would be valuable for deciphering current migratory patterns and anticipating the response of bird species to the ongoing anthropogenic climate and habitat changes.

To date, studies on the origin(s) and evolution(s) of bird migration have largely relied on projecting present-day patterns of biogeography or diversity into the past, through ancestral niche reconstruction (Ponti et al., 2020; Somveille et al., 2020) or ancestral state reconstruction approaches (Dufour et al., 2020). However, this comes with several limitations. First, biotic factors are difficult to assess in deep geological time, and are therefore only partially or not at all considered when inferring past ecological niches. Second, extant life on Earth is a biased sample of all the diversity of life that has existed through geological time (Raup, 1994). Therefore, modelling ancestral states and ancestral ecological niches without integrating fossil evidence significantly reduces inference performance (Finarelli & Flynn, 2006; Meseguer et al., 2015; Lloyd & Slater, 2021). This is particularly true for highly labile traits such as bird migration, which can appear or disappear multiple times independently within a lineage (Berthold et al., 1992; Bearhop et al., 2005; Zink, 2011).

However, whether the avian fossil record can provide insights into past migratory behaviours remains underexplored. The biogeographic distribution of fossils has often been misinterpreted in the literature as evidence for the spatiotemporal origins of migratory behaviour within lineages, while it only provides insights into the geographic origins of lineages that are migratory today (Bell, 2005). In other words, “fossil birds may indicate where species were present, but not if they migrated”, reinforcing the idea that “migratory behaviour is not recorded in the [avian] fossil record” (Somveille et al., 2020). However, this overlooks the fact that well-preserved fossil material can be vector of palaeoecological information, beyond biogeographic considerations. Notably, chemical elements in hard tissues can preserve their pristine stable isotope compositions during the fossilisation process (Iacumin et al., 1996), and some stable isotopes constitute climatic and/or spatial proxies that appear particularly interesting when it comes to track the diverse habitats experienced by migratory animals over their lifetimes.

In terrestrial vertebrates, the stable isotope compositions of soft and hard tissues, such as bones, feathers and teeth, are predominantly influenced by the individual’s diet. For wild obligate drinkers, the oxygen and hydrogen isotopes in tissues are largely derived from drinking water reservoirs (e.g., rivers, ponds, lakes, snowpacks; Longinelli, 1984). These freshwater reservoirs originate from meteoric waters collected at a local or regional scales, whose isotopic compositions vary with latitude in response to climatic factors such as air temperature and precipitation (Dansgaard, 1964). Investigating stable isotopes that reflect such spatial patterns, protocols have been developed for inferring the movements of extant and past vertebrates from the isotopic composition of their biological remains. These protocols typically rely on tissues with incremental or seasonal deposition patterns that can be easily calibrated over time. However, such tissues are either absent (e.g. teeth, Beard & Johnson, 2000; tusks, Rowe et al., 2024) or poorly preserved (e.g., feathers, Lott & Smith, 2006; Hobson & Kardynal, 2023) in the Cenozoic avian fossil record, which predominantly consists of bone remains. Additionally, most modern birds, with the exception of a few species (e.g., kiwi), reach adult size in less than one year and thus do not exhibit the incremental deposition of bone tissues observed in most other vertebrates (Chinsamy & Elzanowski, 2001).

In many vertebrates, linking stable isotope ratios of bone samples to specific spatio-temporal deposition contexts is complicated by the remodelling of bone tissues throughout life (de Buffrénil & Quilhac, 2021). In most mammals, bone tissue undergo complete turnovers due to remodelling at relatively high rates; their stable isotope signature is thus assumed to reflect an average of the individual’s last years of life (e.g., 10 years in humans; Dupras & Schwarcz, 2001; Szostek et al., 2015). This only allows the inference of long-term migratory patterns, and only when compared with early-deposited, non-remodelling tissues such as tooth enamel. In birds, however, as in some other vertebrates, some long bones do not remodel as extensively (Starck & Chinsamy, 2002; Currey et al., 2017), allowing certain bone tissues deposited during growth at the breeding site to remain unresorbed over time. Bird bone has therefore the potential to preserve climatic records from distinct spatio-temporal deposition contexts, and this within tissues that are distinguishable under a light microscope. Properly considered, these temporal records could yield valuable insights into seasonal migration, but this has never been investigated to date.

In this study, we evaluate the predictability of bird migratory behaviour based on their bone remains, using a new experimental framework that combines stable isotope and histological analyses of bone samples. Our approach relies on the introduction of a novel categorisation of bone tissues: either as "early bone tissues" (EBT), which are deposited during chick growth until somatic maturity, or as "late bone tissues" (LBT), which result from bone remodelling events predominantly occurring in somatically mature birds and are thus likely to form during migratory stopovers or wintering periods in migratory species. We demonstrate that, under specific sampling protocols, comparing the apatite phosphate oxygen isotope compositions of EBT ($\delta^{18}O_{p,EBT}$) and LBT ($\delta^{18}O_{p,LBT}$) can distinguish migratory birds from sedentary ones, particularly when the migratory birds experienced significant climatic niche shifts between somatically immature and mature stages. This was tested theoretically by modelling tissue-specific $\delta^{18}O_p$ values for sedentary and migratory birds across various habitats, phenologies, and migratory behaviours, and contrasted with experimental results. Finally, we discuss the expected performance of this approach when applied to fossil birds, depending on their paleoclimatic contexts.

2 MATERIAL AND METHODS

2.1 Experimental framework

We describe here a new experimental framework combining $\delta^{18}O_p$ measurements with histological analysis of bone samples, applied to several migratory and sedentary specimens described in (2.1.1), as a case study.

2.1.1 Specimens

We selected nine skeletal specimens from five sedentary and four migratory extant bird species spanning different migration routes and timings between Europe and Africa. Only specimens with a specified deathplace were selected to ascertain that they belonged to strictly migratory populations in case of partial migrant species, and that they were not captive during their lifetimes. All specimens were obtained from the Collections of the Université de Lyon 1 or the Musée des Confluences, with their catalog numbers provided in Table S1. As a sodium perborate treatment was historically performed to clean some skeletal remains from the Collections de l'Université de Lyon 1, we tested – and confirmed – that this treatment did not alter the original $\delta^{18}O_p$ values of the bones sampled (protocol and results detailed in Appendix A.1 and Fig. S1).

2.1.2 Sampling protocol

Without the technical means to sample only LBT patches, which are too small and not easily localisable along the bone diaphysis *a priori* without destructive sampling or synchrotron imaging, each bone sample from an adult bird could be a mix of EBT and LBT, in proportions f_{EBT} and f_{LBT} respectively. The bulk oxygen isotope composition of a sample ($\delta^{18}O_{p,bulk}$) is thus considered as a linear combination of its tissue-specific $\delta^{18}O_p$ values (equation 1). Therefore, we locally sampled bone diaphyses along cross sections using a Dremel© tool with a diamond-coated circular saw, and associated each bone powder sample of non-juvenile bones with an adjacent thin section to measure the sample-specific f_{LBT} and f_{EBT} (2.1.3). All the selected bird species (2.1.1) were chosen large enough to get the minimum 15 mg of bone powder required for the isotopic analysis protocol (2.1.4) within a relatively thin portion of the diaphysis (2-3 mm). The proportion of bone tissue observed on the thin section was thus assumed to be representative of the associated bone powder sample.

$$\delta^{18}O_{p,bulk} = f_{EBT}.\delta^{18}O_{p,EBT} + f_{LBT}.\delta^{18}O_{p,LBT} \quad \text{(eqn 1)}$$

For each individual, we selected a tibiotarsus – known to be relatively rich in remodelled tissues (i.e., LBT) – and an ulna, known to not remodel much at the midshaft level (De Margerie et al., 2004; Chinsamy et al., 2014). Ulnae were sampled only once for the two following reasons. First, f_{LBT} was assumed negligible at the midshaft (with here a median value of 1.1%, Table S1); thus, the mid-ulnar $\delta^{18}O_{p,bulk}$ value was considered as a good estimate of the samples' EBT $\delta^{18}O_p$ value ($\delta^{18}O_{p,EBT}$). Second, $\delta^{18}O_{p,EBT}$ was assumed homogenous at the individual level due to the lack of impact of body heterothermy on the bulk oxygen isotope composition of bone phosphate (control developed in Appendix A.2, Fig. S1), and despite potential slight mineralisation offsets between and within bones of juvenile individuals (Watanabe, 2018; Canoville et al., 2025). Tibiotarsi sampling was repeated up to eight times along the bone diaphysis – depending

on the diaphysis length – to maximise the chances of sampling LBT patches mineralised outside the breeding season (Fig 1a).

2.1.3 Thin section histological analysis

The thin sections were observed under natural and polarized transmitted light using a LEICA DM750P microscope coupled with a LEICA EC3 photo device. All patches of secondary osteons were classified as LBT, with the exception of those (rather exceptional) that are mineralised before somatic maturity in the case of calcium metabolism imbalances or to repair early microfractures. These latter tissues were classified as EBT, if identifiable. All the remaining bone tissues — fibrolamellar complex (i.e. woven bone matrix associated to primary osteons), the inner and outer circumferential layers made of parallel-fibered tissues — were classified as EBT (Fig 1a). These different bone structures were identified following several diagnostic criteria (Ponton et al., 2007; Chinsamy et al., 2014; Mitchell et al., 2017) detailed and illustrated in Supporting Information (Appendix B; Fig S2). Bone tissues surfaces were measured in pixel number using Adobe Photoshop® on composite images of each thin section reconstructed from a dozen photographs using the "Photomerge" tool. For each thin section, we first measured the proportion of LBT (f_{LBT}) occupying the cortical surface, and then deduced the proportion of EBT (f_{EBT}) from the entire cortical surface measured.

2.1.4 Oxygen isotope analysis of bone apatite phosphate

The collected 15 to 20 mg samples of bone powders (2.2.2) were treated following the same wet chemistry protocol first described by Crowson et al. (1991) and modified by Lécuyer et al. (1993). This protocol aims at isolating the phosphate ions fraction from the bone samples, as oxygen isotopes fractionate in a different way between bone phosphate and carbonate relative to body water. Five replicates per sample were prepared by adding 300 to 400 µg of silver phosphate together with 400 µg of pure carbon in silver foil capsules. CO gas formed during the pyrolysis of the capsules performed at 1450 °C using a Elementar vario PYRO cube™ elemental analyser was analysed using an Isoprime™ isotope ratio mass spectrometer. $\delta^{18}O_{p,\,bulk}$ measurements were calibrated against the phosphorite standard NBS120c ($\delta^{18}O_p$ = 21.7 ‰ V-SMOW; Lécuyer et al., 1993), the barium sulfate NBS127 standard ($\delta^{18}O_p$ = 9.3 ‰ V-SMOW; Halas & Szaran, 2001) and in-house made silver phosphate standards (Lécuyer et al., 2019), to control both for instrumental drift and for any bias that might occur during the chemistry protocol. The final $\delta^{18}O_{p,\,bulk}$ value reported for a sample corresponds to the mean corrected value of the five replicates measured. The mean analytical error for all chemistries was estimated at ± 0.22 ‰ V-SMOW. Isotopic compositions are reported in the δ notation relative to V-SMOW standard.

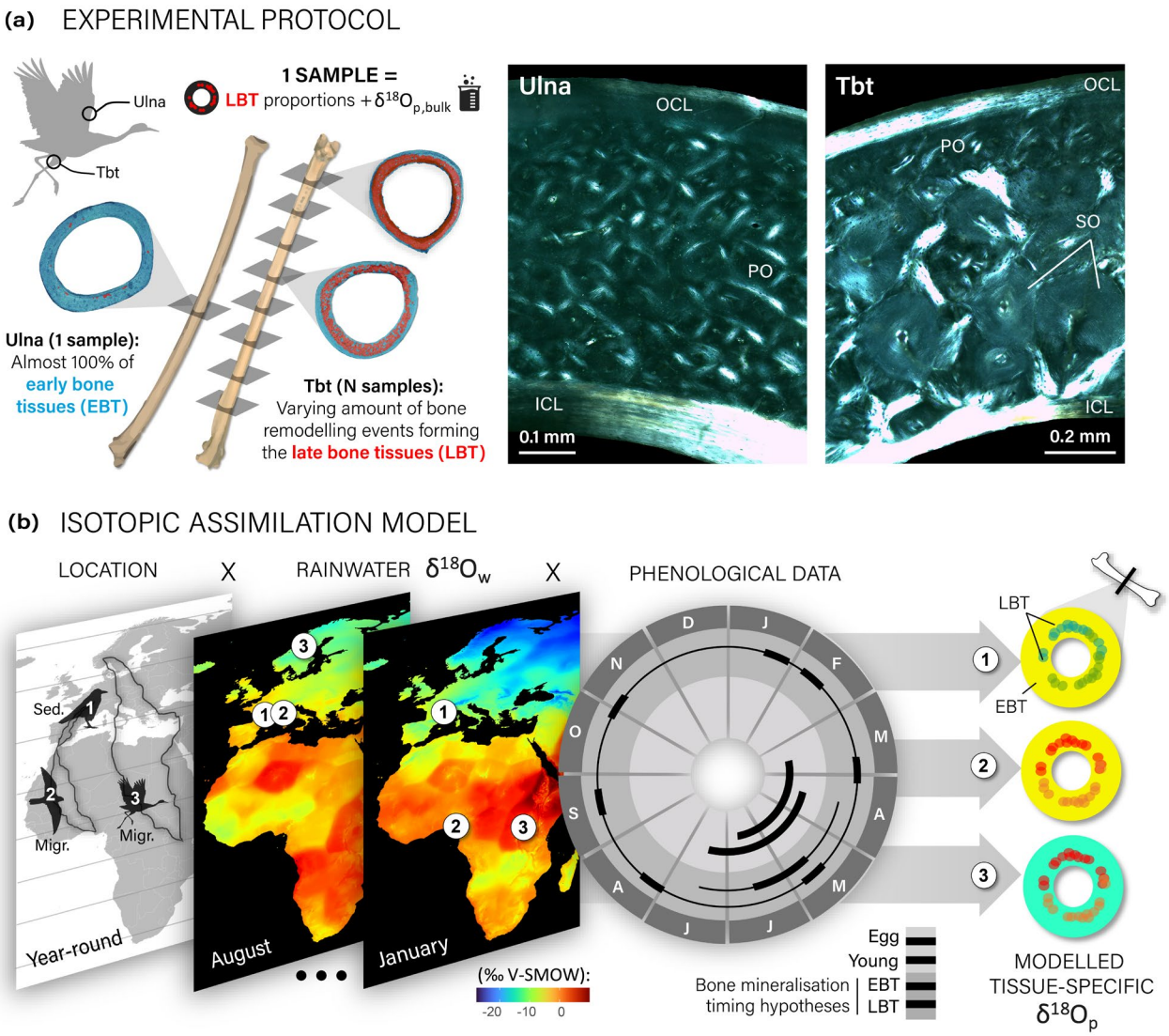

FIGURE 1: Graphical schematics of the experimental (a) and theoretical (b) protocols deciphering oxygen isotope signatures in early bone tissue (EBT) and late bone tissues (LBT). (a) Sampling protocol along the ulna and the tibiotarsus (Tbt), and associated thin sections observed under polarized light to quantify EBT (blue) and LBT (red) proportions. Ulna and Tbt thin sections are from *Circaetus gallicus*, and *Ciconia ciconia* respectively. OCL: outer circumferential layer; ICL: inner circumferential layer, PO: primary osteons; SO: secondary osteons. (b) $\delta^{18}O_w$ values modelled in bird bone tissues depending on the hypothetical annual movements of the bird, its drinking water $\delta^{18}O_w$ value and its species phenological data. Schematic bones are represented in transversal view, with tissues coloured following the $\delta^{18}O_w$ gradient.

2.2 Theoretical framework

We introduce here a theoretical framework that enables the generation of data comparable to those obtained through the experimental approach described above (2.1) – i.e., combinations of bone samples $\delta^{18}O_p$ value and histological composition – for a broad range of sedentary and migratory bird species. Both model implementation and underlying open-access data processing were carried out in R version 4.1.2.

2.2.1 Year-round location data

In order to account for as much variability in extant sedentary birds habitats and phenologies as possible, we drew for 44 sedentary bird species across Europe, western Asia and Africa several plausible living locations from the revised 2023 eBird Basic Dataset (http://www.ebird.org, accessed in February 2024; Sullivan et al., 2009). Each observation drawn from a species-specific database was assumed to be the year-round living location for an individual of that species (Fig. S3). Draws were weighted according to the relative frequency of each country in the species observations, both to

address the over-representation of certain countries in the eBird citizen science programme, and to improve the spatial coverage of draws across the species' living ranges.

In order to account for as much variability in extant bird migratory patterns as possible – i.e. intra- or inter-specific variability in migration timing or routes – the tracking data of 184 individuals from 33 migratory species (Fig. S4) were downloaded from the Movebank database (https://www.movebank.org/, accessed in February 2024). The list of associated references is detailed in Table S1, and, for published works, in the Data Source section. These raw tracking data were subsampled to retain only one spatial coordinate per day over a year. Missing daily locations, often due to interrupted tracking during long stopovers, were filled by the spatial coordinates of the latest available location. Non-overland locations – for which there is no correspondence on land climatic and isotopic maps (2.2.2) – were replaced by the spatial coordinates of the latest overland location, assuming that the water values recorded in bone tissues during these marine flyovers are those derived from the latest land water supply.

2.2.2 Climatic and isotopic data maps

The raster grids of global monthly $\delta^{18}O$ values of precipitation ($\delta^{18}O_w$) and associated standard deviations were extracted from the Waterisotope portal (http://waterisotopes.org, Bowen & Revenaugh, 2003). The raster files of global monthly air temperatures, precipitation amount and associated standard deviations averaged from 1970 to 2000 were extracted from the WorldClim 2.1 database (Fick & Hijmans, 2017). To avoid potential missing values for coastal spatial coordinates (e.g., wetlands), the land-water boundaries of all these raster grids were slightly dilated by averaging the nearest land pixels values using the *focal* function of the *raster* package (Hijmans et al., 2015).

2.2.3 Phenological data and bone deposition timing hypotheses

EBT deposition is assumed to occur from hatching to somatic maturity, with pre-hatching bone fraction neglected for the three following reasons: (i) chicks have very low body weight at birth compared to adults, (ii) pre-hatching tissues of long bones are mostly resorbed during growth in length and diameter (Buffrénil, 2021), and (iii) pre-hatching tissues may have undergone additional oxygen isotope exchange during maternal-to-embryo water exchanges. We assumed that somatic maturity coincides with the attainment of adult body size, which aligns with fledging timing in most bird species (Ricklefs, 1968, 1979; Carrier & Auriemma, 1992). Fledging typically occurs within a month across the range of body sizes in the bird taxa examined in this study (Carrier & Auriemma, 1992; Cooney et al., 2020), and was therefore approximated to 30 days post-hatching across species.

Since hatching dates are unknown, plausible EBT deposition windows were determined for each individual using a 30-day moving window starting within the species-specific hatching date range (Fig. 1b). For each species, plausible hatching dates were estimated by shifting laying periods by the incubation duration, based on phenological data from *Birds of the World* (https://birdsoftheworld.org/bow/home, Billerman et al., 2022). For species with wide breeding ranges, region-specific laying periods were extracted (Table S1). For migratory birds, the 30-days moving window was further constrained to the time period spent on the breeding area.

LBT result from bone remodelling events, forming patches of secondary osteons that are cumulatively deposited in the cortices throughout the bird's lifetime. While the time needed for bone deposition following bone resorption during a bone remodelling event is poorly documented in birds, it is known to depend on the size and metabolic demand of the organism (de Buffrénil & Quilhac, 2021). In cortical bone, deposition lasts only one day in rats and up to 60 to 120 days in humans (Vignery & Baron, 1980). For birds, this duration was approximated to 10 days to provide a conservative estimate, thereby preventing overestimation of the statistical approach's performance (cf. Discussion section, 4.1.3). Accordingly, plausible LBT patches deposition timings were modelled using a 10-day moving window spanning the entire year (Fig. 1b).

2.2.4 Bone samples $\delta^{18}O_{p,bulk}$ modelling

For each individual, plausible $\delta^{18}O_p$ values were calculated through the following steps (Fig. 1b):

(i) *Extraction of $\delta^{18}O_w$ values*: For each daily spatial coordinate (2.2.1), the mean oxygen isotopes ratio in precipitation ($\delta^{18}O_w$) and its standard deviation were extracted from the monthly raster grid (2.2.2). Daily $\delta^{18}O_w$ values experienced by the individual throughout the year were drawn from a normal distribution centred on these means with the corresponding standard deviations.

(ii) *Calculation of tissue-specific $\delta^{18}O_w$ values:* i.e., the mean $\delta^{18}O_w$ of the water consumed during all plausible EBT and LBT deposition periods (2.2.3), yielding plausible $\delta^{18}O_{w,\,EBT}$ and $\delta^{18}O_{w,\,LBT}$ values.

(iii) *Conversion to $\delta^{18}O_p$ values:* In vertebrates, the oxygen from drinking rainwater undergoes several isotopic fractionation events until its incorporation into bone tissues (Luz et al., 1984). Thus, $\delta^{18}O_{w,\,EBT}$ and $\delta^{18}O_{w,\,LBT}$ values were converted into $\delta^{18}O_{p,\,EBT}$ and $\delta^{18}O_{p,\,LBT}$ values using an oxygen isotope fractionation equation between bone phosphate and drinking water, derived from the equation introduced by Amiot et al. (2017) for birds. Since Amiot et al. (2017) fitted an Ordinary Least Square (OLS) regression with $\delta^{18}O_p$ as the independent variable (x) and $\delta^{18}O_w$ as the dependent variable (y), its reciprocal cannot be used for estimating $\delta^{18}O_p$ from $\delta^{18}O_w$ because of residuals that are only minimised for the dependant variable in the OLS framework. Instead, as a first approximate, we estimated $\delta^{18}O_p$ values from a Reduced Major Axis (RMA) regression fitted to Amiot et al. (2017) data (equation 2), which provides a symmetrical fit contrary to the OLS, implemented using the *lmodel2* function from the *lmodel2* R package (Legendre, 2018). A normally distributed error within $\pm\sigma(\varepsilon)$ (the standard deviation of the $\delta^{18}O_p$ residuals from Equation 2, Fig S3) was added to the $\delta^{18}O_p$ estimates.

$$\delta^{18}O_p = 0.75\,\delta^{18}O_w + 20.95 + \varepsilon\,;\; R^2 = 0.699\,;\; \text{pvalue} = 2.35.10^{-06}\,;\; \sigma(\varepsilon) = 1.40\,‰ \qquad \text{(eqn 2)}$$

(iv) *Bone sample simulation:* The $\delta^{18}O_{p,bulk}$ of a bone sample, which is a mix of EBT and LBT, was computed using equation 1, with f_{LBT} randomly sampled within [0,1], and with a $\delta^{18}O_{p,\,EBT}$ value sampled within individual-specific plausible values. The LBT fraction of the bone sample was modelled under two scenarios: either as containing a unique 10-day bone remodelling event (*R*=1), or as containing a number of bone remodelling events between one and five, increasing proportionally with f_{LBT} (*R*=prop.).

2.2.5 Sampling scenarios

Two sampling scenarios were modelled to investigate the predictability of migratory behaviour at either the individual or population level, using a set number *N* of bone samples (*N* = 5, 7, 9, 20 or 100). In the first scenario, all *N* samples are assumed to originate from the same individual and are thus modelled with a unique $\delta^{18}O_{p,\,EBT}$ value (cf. hypotheses in section 2.1.2), calculated from a single 30-day deposition window. The second scenario assumes that the N samples are derived from different individuals of the same species, sharing similar year-round locations, hereafter referred to as a "population". In this case, samples $\delta^{18}O_{p,\,EBT}$ values are modelled from the same tracking data but may correspond to different EBT deposition windows, meaning that $\delta^{18}O_{p,\,EBT}$ values potentially vary among the *N* samples within their plausible range.

3 RESULTS

3.1 Model accuracy depending on oxygen isotope fractionation equation

To test the model accuracy, we simulated all plausible $\delta^{18}O_{p,EBT}$ values for the juvenile and/or sedentary birds sampled (2.1.1), assuming their death sites matched their hatching sites, and all plausible $\delta^{18}O_{p,LBT}$ values for the somatically mature sedentary birds sampled (2.1.1), assuming their death sites represented year-round living locations. These values were obtained following the methodology described in 2.2.4. No $\delta^{18}O_p$ values were modelled for the somatically mature migratory birds sampled due to unknown birthplaces and exact migratory routes. We excluded $\delta^{18}O_{p,LBT}$ computations for samples with less than 20% LBT due to high cumulated errors in equation (1).

The $\delta^{18}O_{p,\,EBT}$ and $\delta^{18}O_{p,\,LBT}$ values modelled using the RMA oxygen isotope fractionation equation fitted on Amiot et al. (2017) data appeared systematically underestimated by ~ 2.5 ‰ compared to control measurements (Fig 2b,c). This was likely due to the original equation being fitted on $\delta^{18}O_p$ measurements of the bones of juvenile chickens raised outdoor, against the mean annual $\delta^{18}O_w$ values in precipitations from the nearest IAEA/WMO stations, rather than *in situ* samplings of drinking water. Hatching dates available in Amiot et al. (2017) indicated that most of these juvenile specimens lived during the season of lowest local $\delta^{18}O_w$ values in precipitations (Table S1), making annual mean $\delta^{18}O_w$ value in precipitations a biased (overestimated) estimate of the bird drinking water $\delta^{18}O_w$. Consequently, the resulting RMA fractionation equation tended to underestimate the $\delta^{18}O_p$ value for a given $\delta^{18}O_w$ value (Fig. 2, b, c).

To address this, we revised Amiot et al. (2017) oxygen isotope fractionation equation by re-estimating juvenile chickens' drinking water $\delta^{18}O_w$ values as the local $\delta^{18}O_w$ in precipitations averaged over the 30 days post-hatching. We first fitted a RMA regression model on the revised data (equation 2b detailed in Fig. S5), that provided improved $\delta^{18}O_{p,\,EBT}$ and $\delta^{18}O_{p,\,LBT}$ estimates compared to equation (2) (Fig. 2). To ensure better calibration against wild birds from various species, we then fitted a RMA regression model on the revised data incorporating to the dataset the measured $\delta^{18}O_{p,}$

$_{EBT}$ values and modelled mean $\delta^{18}O_{w,\ EBT}$ values we obtained for juvenile and sedentary birds. The resulting revised equation (equation 3) provided improved $\delta^{18}O_{p,\ LBT}$ estimates compared to equations 2 and 2b, with experimental data falling within the range of modelled values, though slight underestimation persisted relative to theoretical means for individuals experiencing high $\delta^{18}O_w$ values. Equation 3 was therefore systematically used hereafter for step (iii) of the model implementation (2.2.4).

$$\delta^{18}O_p = 0.61\,\delta^{18}O_w + 20.97 + \varepsilon\,;\ R^2 = 0.647\,;\ \text{pvalue} = 7.32.10^{-07}\,;\ \text{SD}(\varepsilon) = 1.63\ ‰ \qquad \text{(eqn 3)}$$

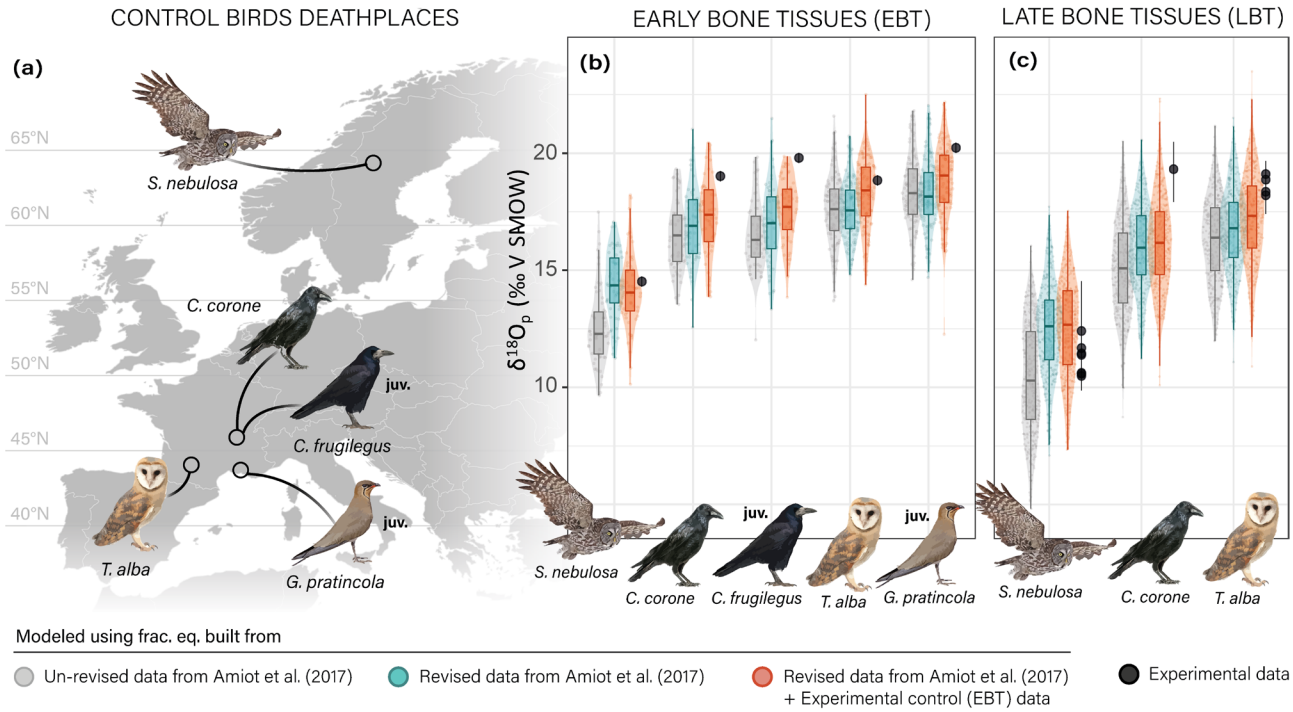

FIGURE 2: For each sedentary and/or juvenile bird sampled: (a), death place; for EBT (b) and LBT (c), comparison of experimental tissue-specific $\delta^{18}O_p$ values with the distribution of plausible tissue-specific $\delta^{18}O_p$ values modelled using either unrevised (equation 2), revised (equation 2b, Fig S5) or revised and extended (equation 3) fractionation equations. Each modelled $\delta^{18}O_{p,EBT}$ value represents a 30-day growth window, while each modelled $\delta^{18}O_{p,LBT}$ value represents a 10-day bone remodelling event. Each experimental $\delta^{18}O_{p,EBT}$ value is derived from a single bone sample and associated thin section. Error bars on experimental $\delta^{18}O_{p,EBT}$ values (smaller than dots' sizes) show mean analytical error for mid-ulnae $\delta^{18}O_{p,bulk}$ measurements. Error bars on $\delta^{18}O_{p,LBT}$ values reflect propagated mean analytical error from $\delta^{18}O_{p,bulk}$ to $\delta^{18}O_{p,LBT}$ via equation (4). Juvenile specimens are marked as "juv.".

3.2 Contrasting $\delta^{18}O_{p,\ EBT}$ and $\delta^{18}O_{p,\ LBT}$ values

3.2.1 Theoretical tissue-specific climatic pattern

To evaluate whether migratory birds can be distinguished from sedentary birds based on their EBT and LBT $\delta^{18}O_p$ values, it is essential to assess how climatic conditions vary across life cycles, and how well $\delta^{18}O_p$ values reflect these patterns.

In both temperate sedentary birds (25°–67° latitude) and migratory birds, chick growth was highly seasonal, predominantly occurring between April and August (Fig. 3a). In temperate latitudes, this period coincided with the onset of warmer season and an increase in local $\delta^{18}O_w$ in precipitation (Fig. 3a). Consequently, modelled $\delta^{18}O_p$ values for temperate sedentary birds were, on average, equal to or lower in LBT than in EBT (Fig. 4; Fig. 5a). A similar pattern was observed in migratory birds that travel short latitudinal distances (0°–15° latitude) or migrate longitudinally (e.g., Richard's Pipit, *Anthus richardi*, Fig. S4), which winter in climates resembling their breeding zones (Figs. 3b-5b).

In contrast, migratory birds travelling longer latitudinal distances (15°–102° latitude) tended to encounter warmer, and occasionally drier, conditions during non-breeding periods (Fig. 3b). For species such as the Common Ringed Plover (*Charadrius hiaticula*) or Sabine's Gull (*Xema sabini*), temperature differences between breeding and non-

breeding periods can reach up to ~35°C. These conditions resulted in higher $\delta^{18}O_w$ during non-breeding periods, leading to modelled $\delta^{18}O_p$ values that were, on average, higher in LBT than in EBT (Figs. 4-5b). A similar pattern was observed in some tropical sedentary birds (~25° to -35° latitude; Fig. 4-5a), where hatching was less seasonal and likely to occur during the late rainy season, when $\delta^{18}O_w$ in precipitation was lower (Fig. 3a).

In temperate sedentary species, only individuals that hatched very early in the breeding season, as early as February-March in some species, exhibited slightly higher average $\delta^{18}O_w$ values year-round compared to those observed during the growth period (Fig. 3a). This pattern was observed in 6.4% of individuals and 1.2% of populations (Fig. 4). The resulting positive average difference between $\delta^{18}O_{p,\,LBT}$ and $\delta^{18}O_{p,\,EBT}$ values was noted in 30% of individuals when $\delta^{18}O_p$ estimates accounted for residuals in equation 3 (Fig. 4), while this outcome remained marginal at the population level, occurring in less than 2,7% of populations, regardless of residuals.

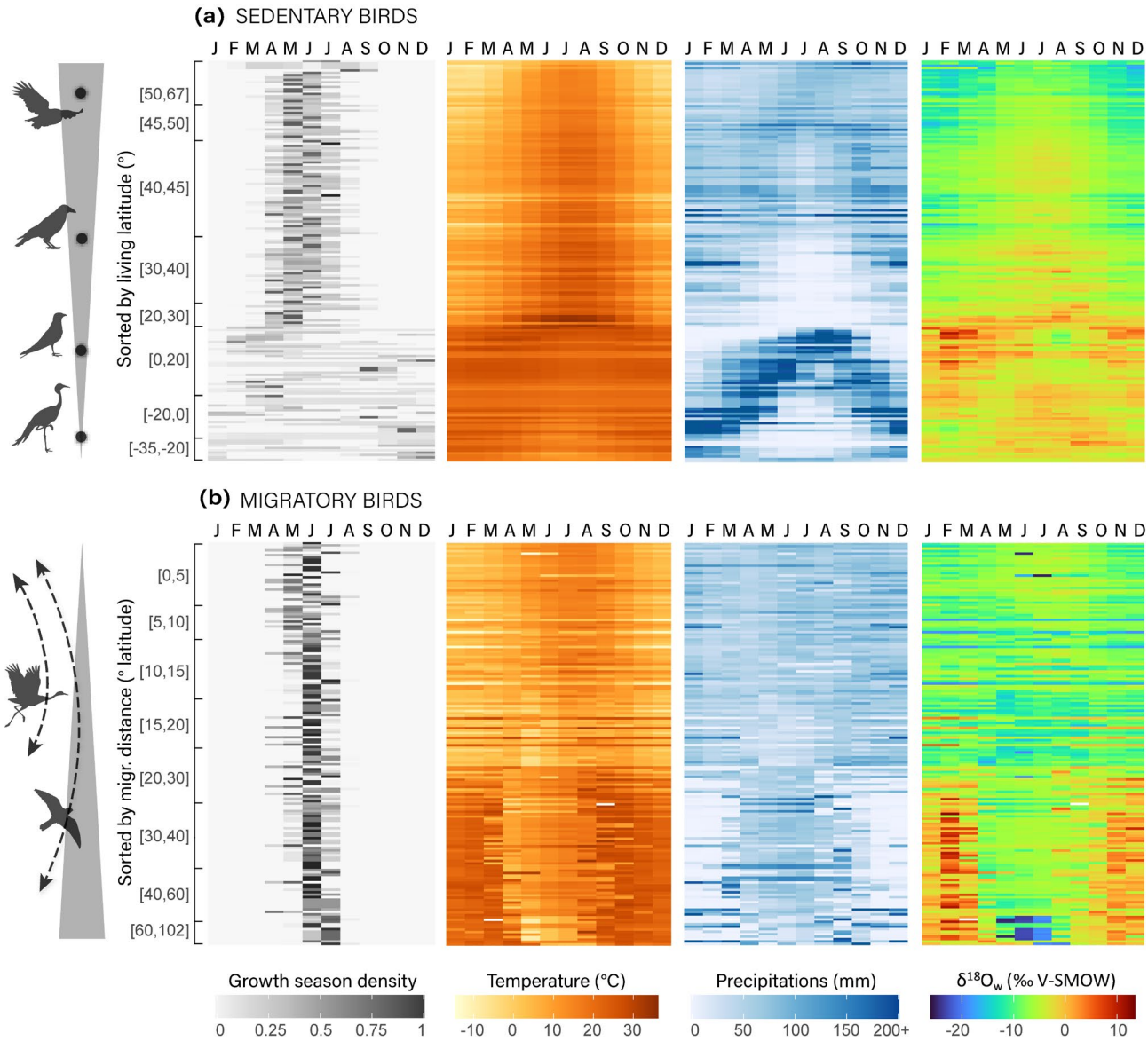

FIGURE 3: Mean monthly climatic variables (temperatures, precipitation amount and precipitations $\delta^{18}O_w$) theoretically experienced by sedentary or migratory populations along a year (from January to December), based on their year-round spatial coordinates (Fig. S3-S4), compared to the local growth season density of their species. Each raw represents a population (i.e., individuals of the same species sharing similar year-round coordinates), with sedentary populations sorted by living latitude (a), and migratory populations sorted by migratory distance (in degrees latitude) (b).

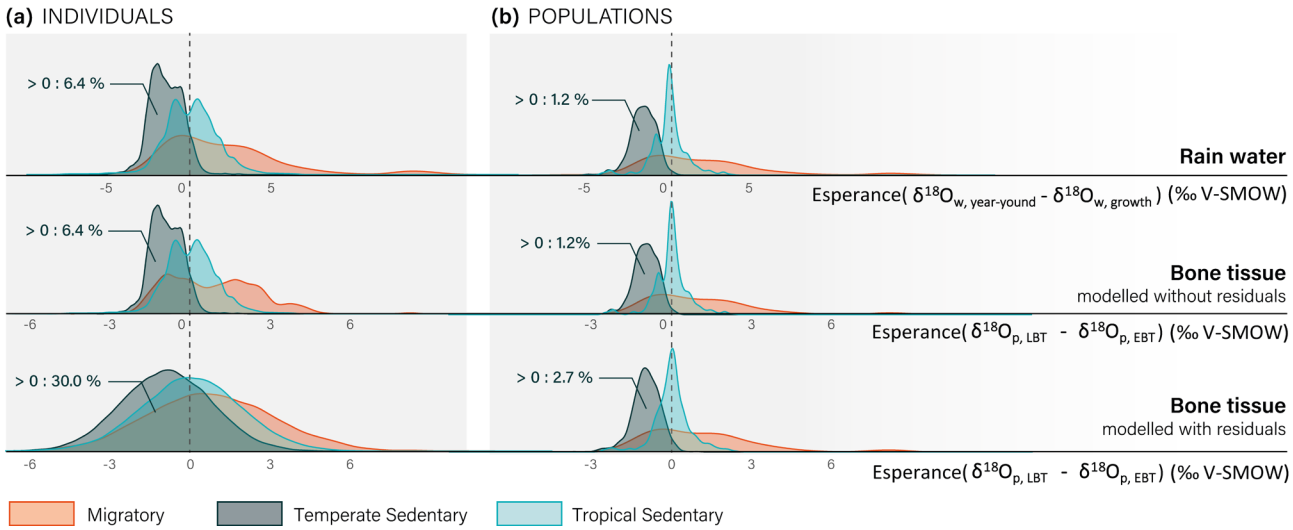

FIGURE 4: Theoretical contrasts between $\delta^{18}O_w$ values of year-round and growth-period rainwater, and the resulting $\delta^{18}O_p$ contrasts expected in bone tissues deposited during these periods (LBT and EBT, respectively), depending on the type of migratory behaviour. These contrasts are shown for (a) individuals and (b) populations (i.e., averaged over individuals of the same species sharing similar year-round locations but with different birth timings). $\delta^{18}O_p$ values were estimated using equation 3, with or without normally distributed error within ±σ(ε) (the standard deviation of $\delta^{18}O_p$ residuals from equation 3).

3.2.2 Predictability of migratory behaviour in case of bulk sampling

Since calculating $\delta^{18}O_{p,\ LBT}$ from $\delta^{18}O_{p,\ bulk}$, $\delta^{18}O_{p,\ EBT}$ and f_{LBT} measurements using equation 1 introduced substantial uncertainty for samples with low f_{LBT} values (Table S1), we instead investigated whether migratory individuals or populations could be distinguished from sedentary ones through the correlation between their $\delta^{18}O_{p,bulk}$ and f_{LBT} values. Given that linear correlations were not expected due to potential intra- or inter-individual variability in $\delta^{18}O_{p,\ LBT}$ values, Spearman's rank correlation coefficient (ρ) was used to quantify the direction and strength of this correlation across N-combinations of bone samples. Each combination was resampled 100 times per population.

Regardless of sampling strategy (individual vs. population; see 2.2.4), sampling effort (number of samples, N) and the hypothesised number of bone remodelling events per sample (R), significantly positive correlations (i.e., ρ>0 and p-value<0.05) between f_{LBT} and $\delta^{18}O_{p,\ bulk}$ were observed in both migratory and tropical sedentary species (Figs. S6-S7). In temperate sedentary species, such correlations were found in approximately 20% of samplings at the individual level but became negligible at the population level as R and N increased (e.g., less than 2.5% of samplings when R=prop and N>20; Fig. S7).

Classifying individuals as migratory based on significantly positive correlations between f_{LBT} and $\delta^{18}O_{p,\ bulk}$ led to notable rate of false positives in temperate and tropical sedentary species, with specificity rates of 92.1% and 81.2%, respectively, when R=prop and N=9 (Figs. 5c-S8). However, applying this decision rule to samplings conducted at the population level minimised the misclassification of temperate sedentary populations as migratory, achieving ~99% specificity across all values of N or R. For migratory populations with strong positive contrasts between LBT and EBT $\delta^{18}O_p$ values, the sensitivity of this test increased with N and R, reaching 100% when R=prop. and N≥20 (Fig. S9).

Conversely, significantly negative correlations (ρ<0 and p-value<0.05) between f_{LBT} and $\delta^{18}O_{p,\ bulk}$ were observed in temperate sedentary birds, some tropical sedentary birds and short distance migratory birds, regardless of sampling or remodelling parameters (Figs. S7-S11). Consequently, using this decision rule to identify birds as sedentary resulted in low specificity, with over 50% of samplings leading to misclassification of short-distance migratory birds as sedentary (Fig. S10). Nonetheless, this decision rule was particularly specific to populations, whether migratory or sedentary, that experienced significantly colder temperatures during growth compared to their lifetime average (Figs. 10-11).

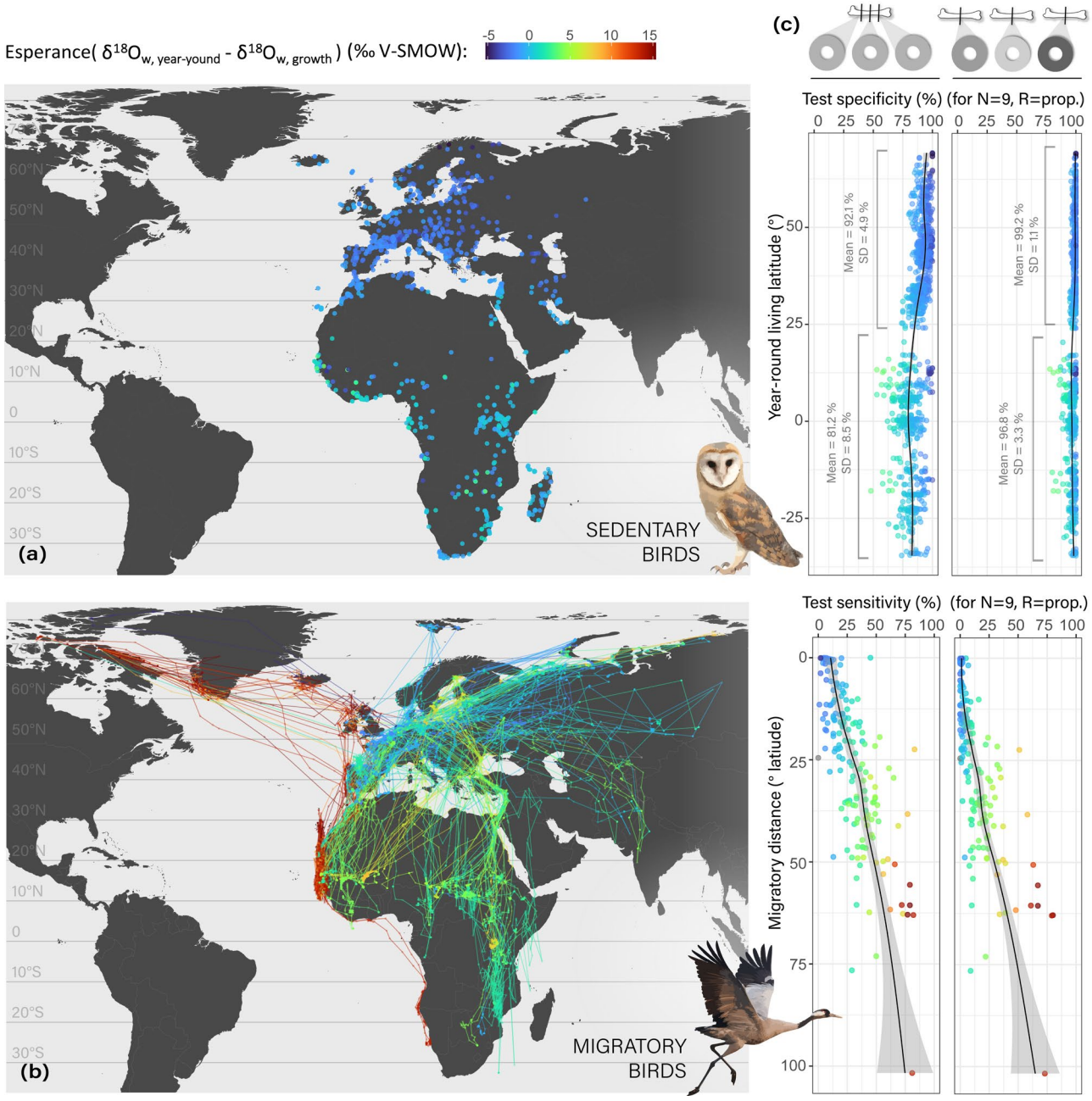

FIGURE 5: (a) Year-round locations of sedentary birds and (b) tracking coordinates of migratory birds coloured according to the population's mean difference between $\delta^{18}O$ values of year-round and growth-period rainwater. (c) Theoretical performance of the test identifying migratory behaviour ("positive" outcome) based on significantly positive correlations between the f_{LBT} and $\delta^{18}O_{p,\ bulk}$ values of samples (i.e., Spearman's ρ>0 and p-value<0.05). This decision rule was applied to samplings of size N=9, conducted either within the same individual (fixed $\delta^{18}O_{p,\ EBT}$ values; left column plots) or within individuals of the same population (varying $\delta^{18}O_{p,\ EBT}$ values; right column plots). Bone samples were modelled to include up to five bone remodelling events (R=prop). N-sized sampling was repeated 100 times per population, allowing the calculation of population-specific specificities (1 – proportion of false positives) and sensitivities (proportion of true positives). Sensitivities and specificities were plotted against the living latitude for sedentary populations, and the latitudinal migratory distance for migratory population, and coloured following the same colour gradient as (a) and (b).

3.2.3 Application case

None of the migratory birds tested within our experimental framework exhibited a significantly increasing trend between its bone samples $\delta^{18}O_{p,bulk}$ values and f_{LBT} values (Table 1). For some individuals, this lack of significance could be attributed to the low variance of $\delta^{18}O_{p,bulk}$ values (e.g., Western Barn Owl, *Tyto alba*) or f_{LBT} values (e.g., Carrion Crow,

Corvus corone). Only the Great Gray Owl (*Strix nebulosa*) demonstrated a significantly decreasing correlation (ρ = -0.93, p-value = $2.94.10^{-4}$).

TABLE 1: For each adult bird sampled, description of the correlation between the percentage of LBT ($100.f_{LBT}$) and the $\delta^{18}O_{p,bulk}$ of the bird's samples. The Spearman's ρ and the p-value of this relationship are to be considered together with the SD of both variables and with the sampling size (N). For each species, the minimum and maximum migratory distances between breeding and wintering latitudes were estimated from eBird data maps (Fig. S12; Sullivan et al., 2009).

Specimen's species	Migratory distance (° latitude)	Number of samples (N)	$\sigma(\delta^{18}O_{p,bulk})$ (‰ V-SMOW)	$\sigma(100.f_{LBT})$ (%)	Spearman's ρ	p-value
Tyto alba	0	6	0.1440	18.8274	0.1739	$7.417.10^{-1}$
Corvus corone	0	5	0.5352	5.3887	0.1000	$9.5000.10^{-1}$
Strix nebulosa	0	9	0.7528	21.4539	-0.9289	**$2.9452.10^{-4}$**
Ciconia ciconia	[15-92]	9	0.4297	21.0098	-0.5000	$1.7766.10^{-1}$
Falco subbuteo	[20-100]	6	0.4800	11.4274	-0.7143	$1.3611.10^{-1}$
Circaetus gallicus	[15-62]	7	0.6368	16.9378	0.0541	$9.0836.10^{-1}$
Grus grus	[15-55]	7	0.6712	23.1151	0.7143	$8.8095.10^{-2}$

3.3 Locally contrasting $\delta^{18}O_{p,EBT}$ values

We tested whether migratory birds that did not hatch on-site (i.e., allochthonous individuals) but originated from significantly different climatic conditions could be distinguished from local birds. This analysis was applied to migratory birds from the experimental case study, classified as migratory if the $\delta^{18}O_p$ values from their EBT-rich bone samples fell outside the 95% confidence interval of the theoretical or empirical $\delta^{18}O_{p,EBT}$ distributions for local birds. Empirical distributions were derived from ulnar mid-shaft or tibiotarsi samples with over 80% EBT content, while theoretical distributions were estimated from the $\delta^{18}O_{p,EBT}$ values modelled for local sedentary birds observed in the wild (see section 2.2.1).

The theoretical distributions showed lower variance at temperate latitudes compared to tropical ones and the empirical distribution exhibited less variance than the theoretical one (Fig 6a). Among the three migratory birds found dead in Southern France, only *G. grus* was located outside its breeding area (Fig. S12). *G. grus* exhibited a $\delta^{18}O_{p,EBT}$ value (13.6‰ V-SMOW) outside the 95% confidence intervals of both control distributions. This value closely matched theoretical expectations for northern breeding areas, such as Scandinavia (Fig. 6a-c), aligning with the species' documented breeding range (Fig. S12). The Short-toed Snake Eagle (*Circaetus gallicus*) and the Eurasian Hobby (*Falco subbuteo*) exhibited $\delta^{18}O_{p,EBT}$ values within the local distributions, suggesting they were either born at their death site or in regions with similar climatic conditions. Lastly, while *C. ciconia* cannot have been born in Ivory Coast in the wild given its species distribution (Fig. S12), it could not be classified as allochthonous with 95% confidence, as its $\delta^{18}O_{p,EBT}$ value fell within the theoretical distribution for its death site (Fig. 6b).

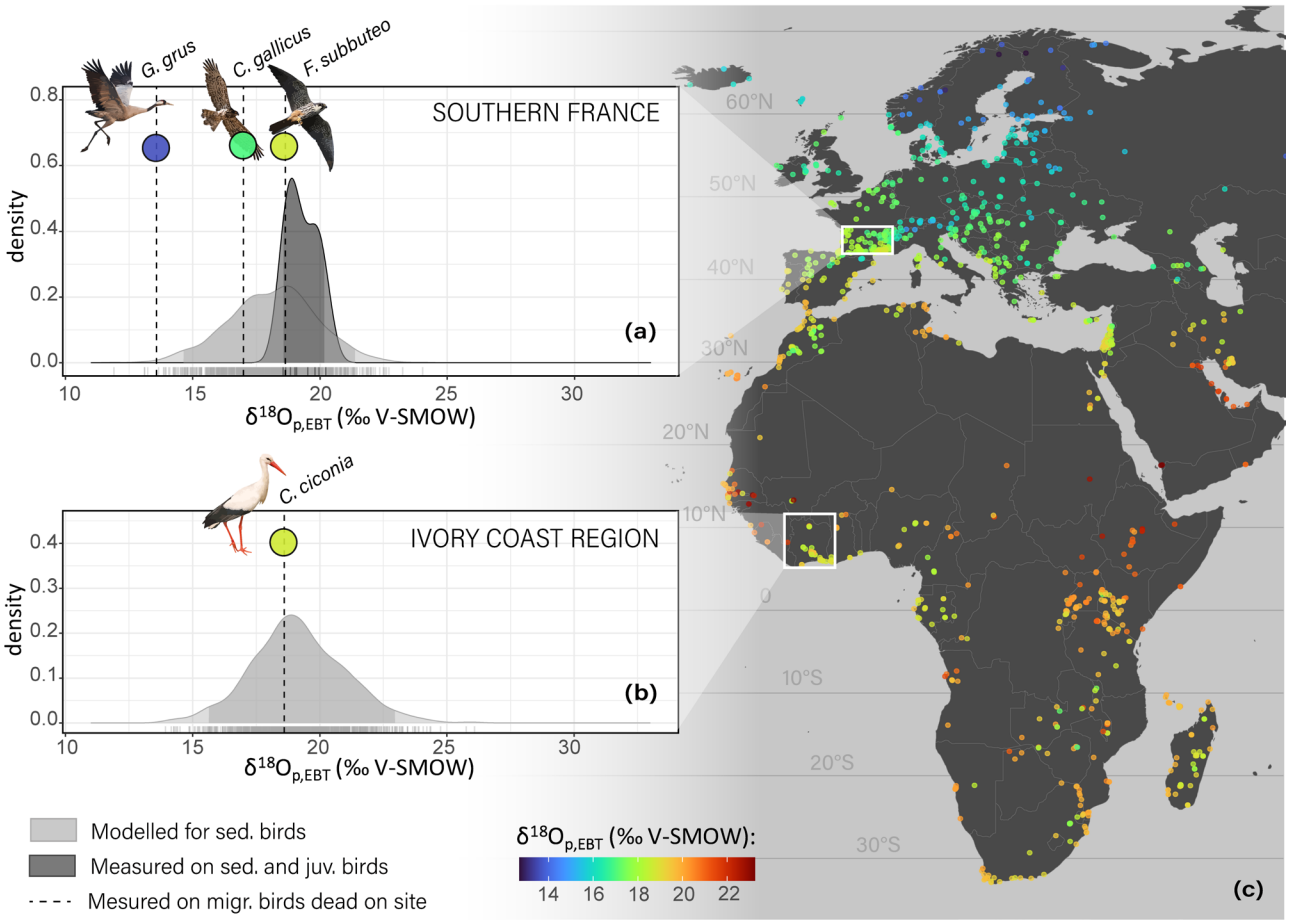

FIGURE 6: Among migratory birds whose remains were found in either Southern France (a) or in Ivory Coast (b), identification of individuals with $\delta^{18}O_{p,EBT}$ values falling outside the 95% confidence interval of the theoretical and/or empirical $\delta^{18}O_{p,EBT}$ distributions of local birds (sedentary and/or juveniles, see 2.3). The 95% confidence interval has a darker shade within each distribution. The dots in (c) illustrate the locations of each modelled population, coloured following its mean $\delta^{18}O_{p,EBT}$ value.

4 DISCUSSION

The origin and evolution of bird seasonal migratory behaviour remain poorly understood. While fossils have the potential to provide the most direct evidence of past migration, no methods currently allow the prediction of migratory behaviour from fossilised bird remains. To our knowledge, this study is the first to investigate the predictability of bird migratory behaviour using stable isotope ratios in bone tissues, signatures that can persist through fossilisation. By combining $\delta^{18}O_p$ measurements with histological analyses that distinguish bone tissues mineralised before somatic maturity or throughout life (early bone tissue, EBT, vs. late bone tissue, LBT), we demonstrated that migratory behaviour can be inferred under specific sampling protocol and assumptions, provided that the birds experienced sufficient seasonal climatic contrasts. We discuss below the assumptions underlying this approach and its applicability to deep-time material.

4.1 What do bone tissues record?

The key considerations of our study align closely with those commonly addressed in isotope-based investigations of the geographic origin of extant migratory birds (Wunder & Norris, 2019). Do the isotope ratios of interest exhibit geographic variation relevant to our research question, given the temporal resolution of the analysed tissues? Can this signature be reliably recovered from these tissues? These questions converge here on a broader issue: what information do bone tissues record? We here identify sources of variability in both isotopic inputs and derived bone tissues, and discuss how sampling strategies can help mitigate this variance to maximise classification accuracy.

4.1.1 Predictability from rainwater oxygen isotopes

Climatic signatures, both geographic and seasonal, are intrinsically embedded in rainwater $\delta^{18}O_w$ values (Dansgaard, 1964). We illustrated that two complementary approaches allowed us to identify specific migratory behaviours based on the $\delta^{18}O_w$ values of water metabolised by the bird during its EBT and LBT deposition timings (i.e., growth and lifetime, respectively), even when accounting for monthly and interannual variation in rainwater $\delta^{18}O_w$ values.

(i) **Testing for climatic niche contrasts:** By contrasting the mean $\delta^{18}O_w$ value of water metabolised throughout a bird's lifetime with those encountered during growth, we emphasised that "niche-switching" migratory birds, which winter in warmer climates than their breeding range (typical of most migratory birds; Dufour et al., 2020), can be distinguished from temperate sedentary birds, which, oppositely, generally experience warmer conditions during growth. However, "Niche-switching" migratory birds cannot be reliably distinguished from tropical sedentary birds born near the wet season. "Niche-tracking" migratory birds, i.e., those following consistent climatic conditions year-round, cannot be differentiated from sedentary birds living in regions with low climate seasonality. Lastly, migratory birds wintering in colder climates (e.g., short-distance, longitudinal, or possibly some altitudinal migrants, not illustrated here) are indistinguishable from sedentary birds living in temperate climates or experiencing cooler non-breeding temperatures in subtropical or tropical regions.

(ii) **Testing for allochthony:** At the site level, if a bird is known to have ingested waters during its growth with $\delta^{18}O_w$ values that differ significantly from the $\delta^{18}O_w$ values of the local growth season, it can be identified as allochthonous to the site. This suggests that the bird was born in a significantly colder climate and migrated to join the site.

4.1.2 "Birds are not rain gauges"

However, as aptly stated by Wunder and Norris (2019): "birds are not rain gauges". Even though the oxygen isotope compositions of terrestrial vertebrate tissues tend to linearly reflect local rainwater $\delta^{18}O_w$ values, this relationship is confounded by numerous unmeasured processes likely to vary within the same individual (i.e., between tissues or within the same tissue over time), between individuals, populations or species (Koch, 1998; Bowen & West, 2019; Hu et al., 2023). The sources of variability primarily stem from physiological factors (e.g., age, sex, metabolic rate), ecological factors (e.g., foraging ecology determining water intake sources), and abiotic factors such as water reservoirs turnover rate, enrichment of heavy isotopes in evaporated water reservoirs (Bowen & West, 2019).

In this study, we estimated the amplitude of this variability from the residuals of a revised oxygen isotope fractionation equation between rainwater and bird bone apatite phosphate, derived from the dataset of Amiot et al. (2017). Both tests described in 4.1.1 were applied to modelled tissue-specific $\delta^{18}O_p$ values accounting for this variability. Although only a small subset of temperate sedentary individuals experienced lower $\delta^{18}O_w$ values (i.e., colder climate) during breeding compared to year-round (4.1.1), variance in $\delta^{18}O_p$ estimates led to an overrepresentation of this pattern when investigating isotopic contrast in bone tissues. Temperate sedentary individuals are therefore not distinguishable from "niche switching" migratory individuals with confidence from $\delta^{18}O_p$ contrasts. However, at the population level, such $\delta^{18}O_p$ contrast remains negligible within temperate sedentary birds due to the normally distributed residuals that tend to cancel out when averaged over several individuals. While investigating within-population $\delta^{18}O_p$ contrasts instead of within-individuals contrasts using the "Climatic Niche Contrasts Test" slightly reduces sensitivity for detecting "niche-switching" migratory birds, it considerably enhances specificity (i.e., almost no sedentary birds are misclassified as migratory). This slight decrease in sensitivity can be mitigated by increasing the sampling size, which is not a major limitation when sampling bones from multiple individuals.

It should however be noted that the residuals from the revised isotopic fractionation equation used for data simulation were likely overestimated, as this equation was based on individuals from multiple species, including both captive (from Amiot et al., 2017) and wild birds (from the present study), the latter of which likely exhibit higher metabolic rates (Bowen & West, 2019). To more accurately assess the efficacy of the two tests, tissue-specific $\delta^{18}O_p$ values should ideally be modelled using residuals derived from species- or population-specific isotopic fractionation equations, which are currently lacking in the literature. Lower residuals in these equations would enhance the theoretical resolution and accuracy of both tests, reducing the sampling sizes required to achieve sufficient specificity and sensitivity.

4.1.3 On bone deposition timing

In this study, bone samples $\delta^{18}O_p$ values were modelled assuming that bone remodelling events, resulting in LBT deposition, occur as 10-day intervals randomly distributed over the bird's lifespan, whether migratory or sedentary.

Among other processes, cortical bone remodelling occurs as a reparative response to microcracks caused by biomechanical stress (Lee et al., 2002; Ponton et al., 2007; Mitchell et al., 2017) or as a result of bone resorption triggered by high metabolic demands, such as those following molting in some species (Meister, 1951). Consequently, the possibility of seasonally biased remodelling processes cannot be excluded, and whether such biases would vary across individuals or species with differing physiologies, phenologies or locomotor habits (e.g., migratory versus sedentary) is largely unexplored. A bone remodelling process exclusively biased towards the breeding season seems unlikely given the diversity of underlying factors. Such biases should therefore not undermine the ability to detect migratory behaviour using isotopic contrasts between EBT and LBT but are likely to influence the resolution of the test, either negatively if remodelling tends to be biased towards the breeding season, or positively otherwise. Deviations from the assumed 10-day remodelling duration would, for their part, require adjustment in sampling efforts. Shorter remodelling intervals (<10 days) would necessitate a greater number of samples to accurately capture annual climatic variability, while longer intervals would require fewer samples to achieve comparable performance.

Conversely, the deposition of the bone tissues constituting EBT is well constrained both temporally and spatially, occurring almost exclusively before fledging and within the breeding zone (Carrier & Auriemma, 1992; Cooney et al., 2020). This enables reliable estimations of the individual $\delta^{18}O_{p,\ EBT}$ value directly through the sampling of poorly remodelled bone regions, such as the mid-ulna. Variability in the "Allochthony Test" likely arises primarily from local species' birth timings, which are influenced by climatic cues. Tropical sites exhibit greater growth season variability compared to temperate ones. Increasing sample both within and between species can improve estimates of broader growth season $\delta^{18}O_{p,\ EBT}$ distributions, thereby enhancing the resolution of predictions.

4.2 Transposing this approach to deep time

The tests outlined in Section 4.1 provide a framework for identifying migratory behaviours in extant bird species through $\delta^{18}O$ analysis of bones tissues. However, their application to fossil specimens introduces several critical considerations.

4.2.1 Diagenetic alteration

Fossil bones can be subject to diagenetic alteration, particularly through interactions with meteoric waters during fossilisation, which can modify the original $\delta^{18}O_p$ signatures and potentially undermine the reliability of migratory behaviour predictions. Nonetheless, it has been demonstrated that phosphate apatite can preserve pristine oxygen isotope compositions in fossil teeth and bones dating back to the Mesozoic (Amiot et al., 2011; Angst et al., 2014; Amiot et al., 2017), when birds arose among theropod dinosaurs. Moreover, well-established diagnostic methods (Iacumin et al., 1996; Lécuyer et al., 2003; Pucéat et al., 2004; Zazzo et al., 2004; Kral et al., 2024) can effectively assess and mitigate the impact of such alterations, preserving the integrity of isotopic analyses.

4.2.2 Sampling constraints

The histological analyses required for the “Climatic Niche Contrast Test” can only be reliably conducted on well-preserved three-dimensional bones, which are rarely found in anatomical connexion at fossil sites. Even when found in close proximity, fossil specimens assigned to the same species are typically assumed to represent different individuals. Since the sampling of multiple bones is necessary to achieve sufficient sampling sizes and access both EBT-rich and LBT-rich samples – at least given the precision of the sampling techniques employed in this study – this restricts the “Niche Switch Test” to population-level applications. While population-level sampling for extant specimens can be limited by the scarcity of individuals from the same locality in comparative anatomy collections, as was the case in this study, this is not a significant limitation at many fossil sites, where abundant material from certain species is often available.

The “Allochthony Test” (Section 4.2) relies on accurate controls for local breeding season $\delta^{18}O_w$ values. For fossil sites, these controls can ideally derive from juvenile bones – readily identifiable by their shape and surface texture (Watanabe, 2018) – or from LBT-poor samples of bird species known to be sedentary (e.g., flightless taxa). In some well documented fossil sites, such material is abundant and spans a wide variety of bird species. In the absence of sedentary or juvenile birds, alternative proxies for growth season temperatures, such as the $\delta^{18}O$ of fossil plants or fossils of sedentary and/or juvenile vertebrates (e.g., mammal teeth; Bernard et al., 2009), could theoretically serve as substitutes. However, these alternative proxies would require careful calibration to ensure they reflect geographic and temporal signatures comparable to those recorded in bird bone tissues (Section 4.1.2). Incorporating these proxies would likely introduce additional variability to the local growth season $\delta^{18}O_w$ values, thereby reducing the resolution of the test.

4.2.3 Evolving $\delta^{18}O_w$ isoscapes

As precipitation $\delta^{18}O_w$ isoscapes evolve over geological time in response to changing climatic conditions (Bowen, 2010), prior knowledge of the paleoclimatic and stratigraphic context of the fossil site is required to ensure the effectiveness of the tests. The "Climatic Niche Contrast Test" is primarily suited for fossil sites associated with temperate climates, because although it effectively differentiates "niche-switching" migratory populations from temperate sedentary populations, it cannot distinguish them from tropical sedentary ones with confidence (Section 4.1). Applying this test to tropical contexts would therefore risk significant misclassification of sedentary populations as migratory. Then, both tests – "Climatic Niche Contrast Test" included when performed at the population level – are likely to decrease in resolution if applied to a fossil site exhibiting high stratigraphic uncertainty, especially if it spanned significant climatic changes over its stratigraphic range. Similarly, the resolution of both tests would inevitably decrease if applied to periods with lower global latitudinal $\delta^{18}O_w$ gradients and/or reduced climate seasonality, such as the Miocene Climate Optimum (Herold et al., 2011). These concerns can be mitigated by integrating stratigraphic and paleoclimatic data from existing literature for the relevant geological periods and sites.

4.3 Conclusion and future directions

Overall, combining histological analyses with oxygen isotope analyses of bone tissues provides a reliable tool for predicting migratory behaviours in extant birds and holds significant promise for fossil applications, provided that the palaeoclimatic context is carefully accounted for. For now, this approach provides a predictive power limited to specific migratory behaviours (i.e. "niche-switching" and/or "allochthonous" migratory birds), and an applicability sometimes limited to specific climatic contexts (e.g. temperate climates). Sensitivity could be further improved by adopting a multi-proxy isotopic framework (Wunder & Norris, 2019; Hobson & Kardynal, 2023), while maintaining awareness of the spatio-temporal context of bird bone mineralisation emphasised in this study. In particular, combining a meteoric water-based proxy ($\delta^{18}O$ or $\delta^{2}H$) with another complementary spatial proxy – such as plant-based ($\delta^{13}C$) or bedrock-based ($^{87}Sr/^{86}Sr$) proxies – could enable the identification of migratory behaviours that are not or poorly detected by a $\delta^{18}O$ analysis alone (e.g., "niche-tracking" migratory birds).

Applied to fossil specimens from sites spanning the Cenozoic, this approach could be key to unravelling the origin(s) and evolution(s) of migratory behaviour in birds, particularly by providing spatiotemporal snapshots of past migratory behaviours that would enable the calibration of methods of ancestral state or niche reconstruction across the phylogeny of birds. More broadly, this study establishes a framework for inferring migratory behaviour in any vertebrate, based on non-fully remodelling biomineralized remains, whether extant or fossilised.

Author contributions

AD, AL, RA, AVL designed the project. AD, RA, AVL and FF acquired the data. AD, RA, and AC analysed the experimental data. AD and JJ designed the theoretical model and statistical analyses. AD wrote the first draft. All authors contributed to revisions.

Acknowledgements

This research received funding from the CNRS-INSU TelluS-INTERRVIE programme in 2022 ("IsoMig" project) and 2023 ("E-VOL" project). The authors would like to thank the following people for their valuable contributions, despite the difficulties caused by the Covid crisis: Emmanuel Robert and Didier Berthet for providing access to the extant and/or fossil specimens from the Université de Lyon 1 and the Musée des Confluences respectively; Colette Guilbaud, Christophe Névado and Doriane Delmas for the preparation of thin sections; Magali Séris for completing the preparation of some chemically treated samples; Vivian de Buffrénil and Jessica Mitchell for providing advice on bird bone histology.

Data availability

All data necessary for the reproducibility of this study—including R scripts, theoretical and experimental datasets—are available in the following Zenodo repository:
https://doi.org/10.5281/zenodo.14825377

Conflict of interests

The authors declare no conflict of interest.

Statement of inclusion

In this study, we focus primarily on the African-European geographic domain, both for skeletal specimens access (experimental approach) and computational time (theoretical approach) convenience. Future research could extend this work by incorporating data from other regions, further enhancing the global perspective we seek to achieve.

REFERENCES

Alerstam, T., Hedenström, A., & Åkesson, S. (2003). Long-distance migration: Evolution and determinants. *Oikos*, *103*(2), 247–260. https://doi.org/10.1034/j.1600-0706.2003.12559.x

Amiot, R., Angst, D., Legendre, S., Buffetaut, E., Fourel, F., Adolfssen, J., André, A., Bojar, A. V., Canoville, A., Barral, A., Goedert, J., Halas, S., Kusuhashi, N., Pestchevitskaya, E., Rey, K., Royer, A., Saraiva, A. Á. F., Savary-Sismondini, B., Siméon, J.-L., … Lécuyer, C. (2017). Oxygen isotope fractionation between bird bone phosphate and drinking water. *The Science of Nature*, *104*(5–6), 47. https://doi.org/10.1007/s00114-017-1468-2

Amiot, R., Wang, X., Zhou, Z., Wang, X., Buffetaut, E., Lécuyer, C., Ding, Z., Fluteau, F., Hibino, T., Kusuhashi, N., Mo, J., Suteethorn, V., Wang, Y., Xu, X., & Zhang, F. (2011). Oxygen isotopes of East Asian dinosaurs reveal exceptionally cold Early Cretaceous climates. *Proceedings of the National Academy of Sciences*, *108*(13), 5179–5183. https://doi.org/10.1073/pnas.1011369108

Angst, D., Lécuyer, C., Amiot, R., Buffetaut, E., Fourel, F., Martineau, F., Legendre, S., Abourachid, A., & Herrel, A. (2014). Isotopic and anatomical evidence of an herbivorous diet in the Early Tertiary giant bird Gastornis. Implications for the structure of Paleocene terrestrial ecosystems. *Naturwissenschaften*, *101*(4), 313–322. https://doi.org/10.1007/s00114-014-1158-2

Beard, B. L., & Johnson, C. M. (2000). Strontium Isotope Composition of Skeletal Material Can Determine the Birth Place and Geographic Mobility of Humans and Animals. *Journal of Forensic Sciences*, *45*(5), 1049–1061. https://doi.org/10.1520/JFS14829J

Bearhop, S., Fiedler, W., Furness, R. W., Votier, S. C., Waldron, S., Newton, J., Bowen, G. J., Berthold, P., & Farnsworth, K. (2005). Assortative Mating as a Mechanism for Rapid Evolution of a Migratory Divide. *Science*, *310*(5747), 502–504. https://doi.org/10.1126/science.1115661

Bell, C. P. (2005). The origin and development of bird migration: Comments on Rappole and Jones, and an alternative evolutionary model. *Ardea*, *93*, 115–123.

Bernard, A., Daux, V., Lécuyer, C., Brugal, J.-P., Genty, D., Wainer, K., Gardien, V., Fourel, F., & Jaubert, J. (2009). Pleistocene seasonal temperature variations recorded in the δ18O of Bison priscus teeth. *Earth and Planetary Science Letters*, *283*(1), 133–143. https://doi.org/10.1016/j.epsl.2009.04.005

Berthold, P., Helbig, A. J., Mohr, G., & Querner, U. (1992). Rapid microevolution of migratory behaviour in a wild bird species. *Nature*, *360*(6405), Article 6405. https://doi.org/10.1038/360668a0

Billerman, S. M., Keeney, K., Rodewald, P. G., & Schulenberg, T. S. (2022). *Birds of the World. Cornell Laboratory of Ornithology, Ithaca, NY, USA.* https://birdsoftheworld.org/bow/home

Bowen, G. J. (2010). Isoscapes: Spatial Pattern in Isotopic Biogeochemistry. *Annual Review of Earth and Planetary Sciences*, *38*(Volume 38, 2010), 161–187. https://doi.org/10.1146/annurev-earth-040809-152429

Bowen, G. J., & Revenaugh, J. (2003). Interpolating the isotopic composition of modern meteoric precipitation. *Water Resources Research*, *39*(10), 2003WR002086. https://doi.org/10.1029/2003WR002086

Bowen, G. J., & West, J. B. (2019). Chapter 3—Isoscapes for Terrestrial Migration Research. In K. A. Hobson & L. I. Wassenaar (Eds.), *Tracking Animal Migration with Stable Isotopes (Second Edition)* (pp. 53–84). Academic Press. https://doi.org/10.1016/B978-0-12-814723-8.00003-9

Buffrénil, V. de (Ed.). (2021). *Vertebrate skeletal histology and paleohistology* (First editon). CRC Press, Taylor & Francis Group. https://doi.org/10.1201/9781351189590

Canoville, A., Robin, J.-P., & de Buffrénil, V. (2025). Ontogenetic development of limb bone microstructure in the king penguin, Aptenodytes patagonicus (Miller, 1778), with considerations for palaeoecological inferences in Sphenisciformes. *Zoological Journal of the Linnean Society*, *203*(1), zlae002. https://doi.org/10.1093/zoolinnean/zlae002

Carrier, D., & Auriemma, J. (1992). A developmental constraint on the fledging time of birds. *Biological Journal of the Linnean Society*, *47*(1), 61–77. https://doi.org/10.1111/j.1095-8312.1992.tb00656.x

Chinsamy, A., Buffetaut, E., Canoville, A., & Angst, D. (2014). Insight into the growth dynamics and systematic affinities of the Late Cretaceous Gargantuavis from bone microstructure. *Naturwissenschaften*, *101*(5), 447–452. https://doi.org/10.1007/s00114-014-1170-6

Chinsamy, A., & Elzanowski, A. (2001). Evolution of growth pattern in birds. *Nature*, *412*(6845), 402–403. https://doi.org/10.1038/35086650

Cooney, C. R., Sheard, C., Clark, A. D., Healy, S. D., Liker, A., Street, S. E., Troisi, C. A., Thomas, G. H., Székely, T., Hemmings, N., & Wright, A. E. (2020). Ecology and allometry predict the evolution of avian developmental durations. *Nature Communications*, *11*(1), 2383. https://doi.org/10.1038/s41467-020-16257-x

Crowson, R. A., Showers, W. J., Wright, E. K., & Hoering, T. C. (1991). Preparation of phosphate samples for oxygen isotope analysis. *Analytical Chemistry*, *63*(20), 2397–2400. https://doi.org/10.1021/ac00020a038

Currey, J. D., Dean, M. N., & Shahar, R. (2017). Revisiting the links between bone remodelling and osteocytes: Insights from across phyla. *Biological Reviews*, *92*(3), 1702–1719. https://doi.org/10.1111/brv.12302

Dansgaard, W. (1964). Stable isotopes in precipitation. *Tellus*, *16*(4), 436–468. https://doi.org/10.3402/tellusa.v16i4.8993

de Buffrénil, V., & Quilhac, A. (2021). Bone remodeling. In *Vertebrate skeletal histology and paleohistology* (pp. 229–246). CRC Press. https://www.taylorfrancis.com/chapters/edit/10.1201/9781351189590-11/bone-remodeling-vivian-de-buffr%C3%A9nil-alexandra-quilhac

De Margerie, E., Sanchez, S., Cubo, J., & Castanet, J. (2004). Torsional resistance as a principal component of the structural design of long bones: Comparative multivariate evidence in birds. *The Anatomical Record Part A: Discoveries in Molecular, Cellular, and Evolutionary Biology*. https://doi.org/10.1002/ar.a.20141

Dufour, P., Descamps, S., Chantepie, S., Renaud, J., Guéguen, M., Schiffers, K., Thuiller, W., & Lavergne, S. (2020). Reconstructing the geographic and climatic origins of long-distance bird migrations. *Journal of Biogeography*, *47*(1), 155–166. https://doi.org/10.1111/jbi.13700

Dupras, T. L., & Schwarcz, H. P. (2001). Strangers in a Strange Land: Stable Isotope Evidence for Human Migration in the Dakhleh Oasis, Egypt. *Journal of Archaeological Science*, *28*(11), 1199–1208. https://doi.org/10.1006/jasc.2001.0640

Fick, S. E., & Hijmans, R. J. (2017). WorldClim 2: New 1-km spatial resolution climate surfaces for global land areas. *International Journal of Climatology*, *37*(12), 4302–4315. https://doi.org/10.1002/joc.5086

Finarelli, J. A., & Flynn, J. J. (2006). Ancestral State Reconstruction of Body Size in the Caniformia (Carnivora, Mammalia): The Effects of Incorporating Data from the Fossil Record. *Systematic Biology*, *55*(2), 301–313. https://doi.org/10.1080/10635150500541698

Halas, S., & Szaran, J. (2001). Improved thermal decomposition of sulfates to SO2 and mass spectrometric determination of δ34S of IAEA SO-5, IAEA SO-6 and NBS-127 sulfate standards. *Rapid Communications in Mass Spectrometry*, *15*(17), 1618–1620. https://doi.org/10.1002/rcm.416

Herold, N., Huber, M., & Müller, R. D. (2011). Modeling the Miocene Climatic Optimum. Part I: Land and Atmosphere. *Journal of Climate*, *24*(24), 6353–6372. https://doi.org/10.1175/2011JCLI4035.1

Hijmans, R. J., Van Etten, J., Cheng, J., Mattiuzzi, M., Sumner, M., Greenberg, J. A., Lamigueiro, O. P., Bevan, A., Racine, E. B., & Shortridge, A. (2015). Package 'raster.' *R Package*, *734*, 473.

Hobson, K. A., & Kardynal, K. J. (2023). Multi-isotope (δ2H, δ13C, δ15N) feather profiles and morphometrics inform patterns of migratory connectivity in three species of North American swallows. *Movement Ecology*, *11*(1), 48. https://doi.org/10.1186/s40462-023-00412-2

Hu, H., Passey, B. H., Lehmann, S. B., Levin, N. E., & Johnson, B. J. (2023). Modeling and interpreting triple oxygen isotope variations in vertebrates, with implications for paleoclimate and paleoecology. *Chemical Geology*, *642*, 121812. https://doi.org/10.1016/j.chemgeo.2023.121812

Iacumin, P., Bocherens, H., Mariotti, A., & Longinelli, A. (1996). Oxygen isotope analyses of co-existing carbonate and phosphate in biogenic apatite: A way to monitor diagenetic alteration of bone phosphate? *Earth and Planetary Science Letters*, *142*(1), 1–6. https://doi.org/10.1016/0012-821X(96)00093-3

Koch, P. L. (1998). ISOTOPIC RECONSTRUCTION OF PAST CONTINENTAL ENVIRONMENTS. *Annual Review of Earth and Planetary Sciences*, *26*(Volume 26, 1998), 573–613. https://doi.org/10.1146/annurev.earth.26.1.573

Kral, A. G., Geisler, T., Wiedenbeck, M., Guagliardo, P., & Tütken, T. (2024). Phosphate uptake is an essential process for rapid bone mineralization during early diagenesis – evidence from bone alteration experiments. *Geochimica et Cosmochimica Acta*, *375*, 173–185. https://doi.org/10.1016/j.gca.2024.04.004

Lécuyer, C., Bogey, C., Garcia, J.-P., Grandjean, P., Barrat, J.-A., Floquet, M., Bardet, N., & Pereda-Superbiola, X. (2003). Stable isotope composition and rare earth element content of vertebrate remains from the Late Cretaceous of northern Spain (Laño): Did the environmental record survive? *Palaeogeography, Palaeoclimatology, Palaeoecology*, *193*(3–4), 457–471. https://doi.org/10.1016/S0031-0182(03)00261-X

Lécuyer, C., Fourel, F., Seris, M., Amiot, R., Goedert, J., & Simon, L. (2019). Synthesis of In-House Produced Calibrated Silver Phosphate with a Large Range of Oxygen Isotope Compositions. *Geostandards and Geoanalytical Research*, *43*(4), 681–688. https://doi.org/10.1111/ggr.12285

Lécuyer, C., Grandjean, P., O'Neil, J. R., Cappetta, H., & Martineau, F. (1993). Thermal excursions in the ocean at the Cretaceous—Tertiary boundary (northern Morocco): δ18O record of phosphatic fish debris. *Palaeogeography, Palaeoclimatology, Palaeoecology*, *105*(3), 235–243. https://doi.org/10.1016/0031-0182(93)90085-W

Lee, T. C., Staines, A., & Taylor, D. (2002). Bone adaptation to load: Microdamage as a stimulus for bone remodelling. *Journal of Anatomy*, *201*(6), 437–446. https://doi.org/10.1046/j.1469-7580.2002.00123.x

Legendre, P. (2018). *lmodel2: Model II Regression* (Version 1.7-3) [Computer software]. https://cran.r-project.org/web/packages/lmodel2/index.html

Lloyd, G. T., & Slater, G. J. (2021). A Total-Group Phylogenetic Metatree for Cetacea and the Importance of Fossil Data in Diversification Analyses. *Systematic Biology*, *70*(5), 922–939. https://doi.org/10.1093/sysbio/syab002

Longinelli, A. (1984). Oxygen isotopes in mammal bone phosphate: A new tool for paleohydrological and paleoclimatological research? *Geochimica et Cosmochimica Acta*, *48*(2), 385–390.

Lott, C. A., & Smith, J. P. (2006). A Geographic-Information-System Approach to Estimating the Origin of Migratory Raptors in North America Using Stable Hydrogen Isotope Ratios in Feathers. *The Auk*, *123*(3), 822–835. https://doi.org/10.1093/auk/123.3.822

Louchart, A. (2008). Emergence of long distance bird migrations: A new model integrating global climate changes. *Naturwissenschaften*, *95*(12), 1109–1119. https://doi.org/10.1007/s00114-008-0435-3

Luz, B., Kolodny, Y., & Horowitz, M. (1984). Fractionation of oxygen isotopes between mammalian bone-phosphate and environmental drinking water. *Geochimica et Cosmochimica Acta*, *48*(8), 1689–1693. https://doi.org/10.1016/0016-7037(84)90338-7

Meister, W. (1951). Changes in histological structure of the long bones of birds during the molt. *The Anatomical Record*, *111*(1), 1–21. https://doi.org/10.1002/ar.1091110102

Meseguer, A. S., Lobo, J. M., Ree, R., Beerling, D. J., & Sanmartín, I. (2015). Integrating Fossils, Phylogenies, and Niche Models into Biogeography to Reveal Ancient Evolutionary History: The Case of Hypericum (Hypericaceae). *Systematic Biology*, *64*(2), 215–232. https://doi.org/10.1093/sysbio/syu088

Mitchell, J., Legendre, L. J., Lefèvre, C., & Cubo, J. (2017). Bone histological correlates of soaring and high-frequency flapping flight in the furculae of birds. *Zoology*, *122*, 90–99. https://doi.org/10.1016/j.zool.2017.03.004

Ponti, R., Arcones, A., Ferrer, X., & Vieites, D. R. (2020). Lack of evidence of a Pleistocene migratory switch in current bird long-distance migrants between Eurasia and Africa. *Journal of Biogeography*, *47*(7), 1564–1573. https://doi.org/10.1111/jbi.13834

Ponton, F., Montes, L., Castanet, J., & Cubo, J. (2007). Bone histological correlates of high-frequency flapping flight and body mass in the furculae of birds: A phylogenetic approach: EFFECTS OF TYPE OF FLIGHT AND BODY MASS IN THE FURCULAE OF BIRDS. *Biological Journal of the Linnean Society*, *91*(4), 729–738. https://doi.org/10.1111/j.1095-8312.2007.00836.x

Pucéat, E., Reynard, B., & Lécuyer, C. (2004). Can crystallinity be used to determine the degree of chemical alteration of biogenic apatites? *Chemical Geology*, *205*(1), 83–97. https://doi.org/10.1016/j.chemgeo.2003.12.014

Raup, D. M. (1994). The role of extinction in evolution. *Proceedings of the National Academy of Sciences*, *91*(15), 6758–6763. https://doi.org/10.1073/pnas.91.15.6758

Ricklefs, R. E. (1968). Patterns of Growth in Birds. *Ibis*, *110*(4), 419–451. https://doi.org/10.1111/j.1474-919X.1968.tb00058.x

Ricklefs, R. E. (1979). Adaptation, Constraint, and Compromise in Avian Postnatal Development. *Biological Reviews*, *54*(3), 269–290. https://doi.org/10.1111/j.1469-185X.1979.tb01013.x

Rowe, A. G., Bataille, C. P., Baleka, S., Combs, E. A., Crass, B. A., Fisher, D. C., Ghosh, S., Holmes, C. E., Krasinski, K. E., Lanoë, F., Murchie, T. J., Poinar, H., Potter, B., Rasic, J. T., Reuther, J., Smith, G. M., Spaleta, K. J., Wygal, B. T., & Wooller, M. J. (2024). A female woolly mammoth's lifetime movements end in an ancient Alaskan hunter-gatherer camp. *Science Advances*, *10*(3), eadk0818. https://doi.org/10.1126/sciadv.adk0818

Salewski, V., & Bruderer, B. (2007). The evolution of bird migration—A synthesis. *Naturwissenschaften*, *94*(4), 268–279. https://doi.org/10.1007/s00114-006-0186-y

Somveille, M. (2016). The global ecology of bird migration: Patterns and processes. *Frontiers of Biogeography*, *8*(3). https://doi.org/10.21425/F58332694

Somveille, M., Wikelski, M., Beyer, R. M., Rodrigues, A. S. L., Manica, A., & Jetz, W. (2020). Simulation-based reconstruction of global bird migration over the past 50,000 years. *Nature Communications*, *11*(1), 801. https://doi.org/10.1038/s41467-020-14589-2

Starck, J. M., & Chinsamy, A. (2002). Bone microstructure and developmental plasticity in birds and other dinosaurs. *Journal of Morphology*, *254*(3), 232–246. https://doi.org/10.1002/jmor.10029

Sullivan, B. L., Wood, C. L., Iliff, M. J., Bonney, R. E., Fink, D., & Kelling, S. (2009). eBird: A citizen-based bird observation network in the biological sciences. *Biological Conservation*, *142*(10), 2282–2292. https://doi.org/10.1016/j.biocon.2009.05.006

Szostek, K., Mądrzyk, K., & Cienkosz-Stepańczak, B. (2015). Strontium isotopes as an indicator of human migration – easy questions, difficult answers. *Anthropological Review*, *78*(2), 133–156. https://doi.org/10.1515/anre-2015-0010

Vignery, A., & Baron, R. (1980). Dynamic histomorphometry of alveolar bone remodeling in the adult rat. *The Anatomical Record*, *196*(2), 191–200. https://doi.org/10.1002/ar.1091960210

Watanabe, J. (2018). Ontogeny of Surface Texture of Limb Bones in Modern Aquatic Birds and Applicability of Textural Ageing. *The Anatomical Record*, *301*(6), 1026–1045. https://doi.org/10.1002/ar.23736

Wunder, M. B., & Norris, D. R. (2019). Chapter 8—Design and Analysis for Isotope-Based Studies of Migratory Animals. In K. A. Hobson & L. I. Wassenaar (Eds.), *Tracking Animal Migration with Stable Isotopes (Second Edition)* (pp. 191–206). Academic Press. https://doi.org/10.1016/B978-0-12-814723-8.00008-8

Zazzo, A., Lécuyer, C., & Mariotti, A. (2004). Experimentally-controlled carbon and oxygen isotope exchange between bioapatites and water under inorganic and microbially-mediated conditions. *Geochimica et Cosmochimica Acta*, *68*(1), 1–12. https://doi.org/10.1016/S0016-7037(03)00278-3

Zink, R. M. (2011). The evolution of avian migration: THE EVOLUTION OF AVIAN MIGRATION. *Biological Journal of the Linnean Society*, *104*(2), 237–250. https://doi.org/10.1111/j.1095-8312.2011.01752.x

DATA SOURCE

Aikens, E. O., Nourani, E., Fiedler, W., Wikelski, M., & Flack, A. (2024). Learning shapes the development of migratory behavior. *Proceedings of the National Academy of Sciences*, *121*(12), e2306389121. https://doi.org/10.1073/pnas.2306389121

Boiko, D., & Wikelski, M. (2019). Moulting sites of Latvian Whooper Swan Cygnus cygnus cygnets fitted with GPS-GSM transmitters. *Wildfowl*, *0*, Article 0.

Brønnvik, H., Nourani, E., Fiedler, W., & Flack, A. (2024a). Experience reduces route selection for conspecifics by the collectively migrating white stork. *Current Biology*, *34*(9), 2030-2037.e3. https://doi.org/10.1016/j.cub.2024.03.052

Brønnvik, H., Nourani, E., Fiedler, W., & Flack, A. (2024b). Experience reduces route selection for conspecifics by the collectively migrating white stork. *Current Biology*, *34*(9), 2030-2037.e3. https://doi.org/10.1016/j.cub.2024.03.052

Burgess, M. D., Finch, T., Border, J. A., Castello, J., Conway, G., Ketcher, M., Lawrence, M., Orsman, C. J., Mateos, J., Proud, A., Westerberg, S., Wiffen, T., & Henderson, I. G. (2020). Weak migratory connectivity, loop migration and multiple non-breeding site use in British breeding Whinchats Saxicola rubetra. *Ibis*, *162*(4), 1292–1302. https://doi.org/10.1111/ibi.12825

Cerritelli, G., Vanni, L., Baldaccini, N. E., Lenzoni, A., Sorrenti, M., & Giunchi, D. (2023). Trailing the heat: Eurasian teal Anas crecca schedule their spring migration basing on the increase in soil temperatures along the route. *Journal of Avian Biology*, *2023*(9–10), e03122. https://doi.org/10.1111/jav.03122

Cheng, Y., Fiedler, W., Wikelski, M., & Flack, A. (2019). "Closer-to-home" strategy benefits juvenile survival in a long-distance migratory bird. *Ecology and Evolution*, *9*(16), 8945–8952. https://doi.org/10.1002/ece3.5395

Chudzińska, M. E., Nabe-Nielsen, J., Nolet, B. A., & Madsen, J. (2016). Foraging behaviour and fuel accumulation of capital breeders during spring migration as derived from a combination of satellite- and ground-based observations. *Journal of Avian Biology*, *47*(4), 563–574. https://doi.org/10.1111/jav.00899

Curk, T., Kulikova, O., Fufachev, I., Wikelski, M., Safi, K., & Pokrovsky, I. (2022). Arctic Migratory Raptor Selects Nesting Area During the Previous Breeding Season. *Frontiers in Ecology and Evolution*, *10*. https://doi.org/10.3389/fevo.2022.865482

Davidson, S. C., Bohrer, G., Gurarie, E., LaPoint, S., Mahoney, P. J., Boelman, N. T., Eitel, J. U. H., Prugh, L. R., Vierling, L. A., Jennewein, J., Grier, E., Couriot, O., Kelly, A. P., Meddens, A. J. H., Oliver, R. Y., Kays, R., Wikelski, M., Aarvak, T., Ackerman, J. T., … Hebblewhite, M. (2020). Ecological insights from three decades of animal movement tracking across a changing Arctic. *Science*, *370*(6517), 712–715. https://doi.org/10.1126/science.abb7080

Dufour, P., De Franceschi, C., Doniol-Valcroze, P., Jiguet, F., Guéguen, M., Renaud, J., Lavergne, S., & Crochet, P.-A. (2021). A new westward migration route in an Asian passerine bird. *Current Biology*, *31*(24), 5590-5596.e4. https://doi.org/10.1016/j.cub.2021.09.086

Exo, K.-M., Hillig, F., & Bairlein, F. (2019). Migration routes and strategies of Grey Plovers (Pluvialis squatarola) on the East Atlantic Flyway as revealed by satellite tracking. *Avian Research*, *10*(1), 28. https://doi.org/10.1186/s40657-019-0166-5

Flack, A., Fiedler, W., Blas, J., Pokrovsky, I., Kaatz, M., Mitropolsky, M., Aghababyan, K., Fakriadis, I., Makrigianni, E., Jerzak, L., Azafzaf, H., Feltrup-Azafzaf, C., Rotics, S., Mokotjomela, T. M., Nathan, R., & Wikelski, M. (2016). Costs of migratory decisions: A comparison across eight white stork populations. *Science Advances*, *2*(1), e1500931. https://doi.org/10.1126/sciadv.1500931

Giunchi, D., Baldaccini, N. E., Lenzoni, A., Luschi, P., Sorrenti, M., Cerritelli, G., & Vanni, L. (2019). Spring migratory routes and stopover duration of satellite-tracked Eurasian Teals Anas crecca wintering in Italy. *Ibis*, *161*(1), 117–130. https://doi.org/10.1111/ibi.12602

Kays, R., Davidson, S. C., Berger, M., Bohrer, G., Fiedler, W., Flack, A., Hirt, J., Hahn, C., Gauggel, D., Russell, B., Kölzsch, A., Lohr, A., Partecke, J., Quetting, M., Safi, K., Scharf, A., Schneider, G., Lang, I., Schaeuffelhut, F., … Wikelski, M. (2022). The Movebank system for studying global animal movement and demography. *Methods in Ecology and Evolution*, *13*(2), 419–431. https://doi.org/10.1111/2041-210X.13767

Kok, E. M. A., Tibbitts, T. L., Douglas, D. C., Howey, P. W., Dekinga, A., Gnep, B., & Piersma, T. (2020). A red knot as a black swan: How a single bird shows navigational abilities during repeat crossings of the Greenland Icecap. *Journal of Avian Biology*, *51*(8), 1–11. https://doi.org/10.1111/jav.02464

Koks, B., Schlaich, A., Schaub, T., Klaassen, R., Anselin, A., Desmet, P., Milotic, T., Janssens, K., & Bouten, W. (2023). *H_GRONINGEN - Western marsh harriers (Circus aeruginosus, Accipitridae) breeding in Groningen (the Netherlands)* [Dataset]. Research Institute for Nature and Forest (INBO). https://doi.org/10.5281/zenodo.10053658

Kölzsch, A., Bauer, S., de Boer, R., Griffin, L., Cabot, D., Exo, K.-M., van der Jeugd, H. P., & Nolet, B. A. (2015). Forecasting spring from afar? Timing of migration and predictability of phenology along different migration routes of an avian herbivore. *Journal of Animal Ecology*, *84*(1), 272–283.

Kölzsch, A., Müskens, G. J. D. M., Kruckenberg, H., Glazov, P., Weinzierl, R., Nolet, B. A., & Wikelski, M. (2016). Towards a new understanding of migration timing: Slower spring than autumn migration in geese reflects different decision rules for stopover use and departure. *Oikos*, *125*(10), 1496–1507. https://doi.org/10.1111/oik.03121

Kölzsch, A., Müskens, G. J. D. M., Szinai, P., Moonen, S., Glazov, P., Kruckenberg, H., Wikelski, M., & Nolet, B. A. (2019). Flyway connectivity and exchange primarily driven by moult migration in geese. *Movement Ecology*, *7*(1), 3. https://doi.org/10.1186/s40462-019-0148-6

Léandri-Breton, D., Lamarre, J., & Bêty, J. (2019). Seasonal variation in migration strategies used to cross ecological barriers in a nearctic migrant wintering in Africa. *Journal of Avian Biology*, *50*(6), N.PAG-N.PAG. https://doi.org/10.1111/jav.02101

Lisovski, S., Bauer, S., Briedis, M., Davidson, S. C., Dhanjal-Adams, K. L., Hallworth, M. T., Karagicheva, J., Meier, C. M., Merkel, B., Ouwehand, J., Pedersen, L., Rakhimberdiev, E., Roberto-Charron, A., Seavy, N. E., Sumner, M. D., Taylor, C. M., Wotherspoon, S. J., & Bridge, E. S. (2020). Light-level geolocator analyses: A user's guide. *Journal of Animal Ecology*, *89*(1), 221–236. https://doi.org/10.1111/1365-2656.13036

Lisovski, S., Neumann, R., Albrecht, T., Munclinger, P., Ahola, M. P., Bauer, S., Cepak, J., Fransson, T., Jakobsson, S., Jaakkonen, T., Klvana, P., Kullberg, C., Laaksonen, T., Metzger, B., Piha, M., Shurulinkov, P., Stach, R., Ström, K., Velmala, W., & Briedis, M. (2021). The Indo-European flyway: Opportunities and constraints reflected by Common Rosefinches breeding across Europe. *Journal of Biogeography*, *48*(6), 1255–1266. https://doi.org/10.1111/jbi.14085

Maxhuni, Q., Gashi, A., Hoxha, L., Wolf, G., & Fiedler, W. (2021). *Data from: Study "LifeTrack White Stork Kosova."* https://datarepository.movebank.org/handle/10255/move.1339

Meier, C. M., Karaardıç, H., Aymí, R., Peev, S. G., Witvliet, W., & Liechti, F. (2020a). Population-specific adjustment of the annual cycle in a super-swift trans-Saharan migrant. *Journal of Avian Biology*, *51*(11). https://doi.org/10.1111/jav.02515

Meier, C. M., Karaardıç, H., Aymí, R., Peev, S. G., Witvliet, W., & Liechti, F. (2020b). Population-specific adjustment of the annual cycle in a super-swift trans-Saharan migrant. *Journal of Avian Biology*, *51*(11). https://doi.org/10.1111/jav.02515

Meier, C. M., Rime, Y., Lisovski, S., Buchmann, M., & Liechti, F. (2022). Locally adapted migration strategies? Comparing routes and timing of northern wheatears from alpine and lowland European populations. *Journal of Avian Biology*, *2022*(8), e02932. https://doi.org/10.1111/jav.02932

Pedersen, L., Jakobsen, N. M., Strandberg, R., Thorup, K., & Tøttrup, A. P. (2019). Sex-specific difference in migration schedule as a precursor of protandry in a long-distance migratory bird. *The Science of Nature*, *106*(7), 45. https://doi.org/10.1007/s00114-019-1637-6

Piironen, A., Paasivaara, A., & Laaksonen, T. (2021). Birds of three worlds: Moult migration to high Arctic expands a boreal-temperate flyway to a third biome. *Movement Ecology*, *9*(1), 47. https://doi.org/10.1186/s40462-021-00284-4

Pokrovsky, I., Kölzsch, A., Sherub, S., Fiedler, W., Glazov, P., Kulikova, O., Wikelski, M., & Flack, A. (2021). Longer days enable higher diurnal activity for migratory birds. *Journal of Animal Ecology*, *90*(9), 2161–2171. https://doi.org/10.1111/1365-2656.13484

Rueda-Uribe, C., Lötberg, U., Ericsson, M., Tesson, S. V. M., & Åkesson, S. (2021). First tracking of declining Caspian terns Hydroprogne caspia breeding in the Baltic Sea reveals high migratory dispersion and disjunct annual ranges as obstacles to effective conservation. *Journal of Avian Biology*, *52*(9), 1–14. https://doi.org/10.1111/jav.02743

Schwemmer, P., Mercker, M., Vanselow, K. H., Bocher, P., & Garthe, S. (2021a). Migrating curlews on schedule: Departure and arrival patterns of a long-distance migrant depend on time and breeding location rather than on wind conditions. *Movement Ecology*, *9*(1), 9. https://doi.org/10.1186/s40462-021-00252-y

Schwemmer, P., Mercker, M., Vanselow, K. H., Bocher, P., & Garthe, S. (2021b). Migrating curlews on schedule: Departure and arrival patterns of a long-distance migrant depend on time and breeding location rather than on wind conditions. *Movement Ecology*, *9*(1), 9. https://doi.org/10.1186/s40462-021-00252-y

Shariati Najafabadi, M., Darvishzadeh, R., Skidmore, A. K., Kölzsch, A., Vrieling, A., Nolet, B. A., Exo, K.-M., Meratnia, N., Havinga, P. J. M., Stahl, J., & Toxopeus, A. G. (2015). Satellite- versus temperature-derived green wave indices for predicting the timing of spring migration of avian herbivores. *Ecological Indicators*, *58*, 322–331. https://doi.org/10.1016/j.ecolind.2015.06.005

Shariati-Najafabadi, M., Darvishzadeh, R., Skidmore, A. K., Kölzsch, A., Exo, K.-M., Nolet, B. A., Griffin, L., Stahl, J., Havinga, P. J. M., Meratnia, N., & Toxopeus, A. G. (2016). Environmental parameters linked to the last migratory stage of barnacle geese en route to their breeding sites. *Animal Behaviour*, *118*, 81–95. https://doi.org/10.1016/j.anbehav.2016.05.018

Shariatinajafabadi, M., Wang, T., Skidmore, A. K., Toxopeus, A. G., Kölzsch, A., Nolet, B. A., Exo, K.-M., Griffin, L., Stahl, J., & Cabot, D. (2014). Migratory Herbivorous Waterfowl Track Satellite-Derived Green Wave Index. *PLOS ONE*, *9*(9), e108331. https://doi.org/10.1371/journal.pone.0108331

Škrábal, J., Krejčí, Š., Raab, R., Sebastián-González, E., & Literák, I. (2023). Soaring over open waters: Horizontal winds provide lift to soaring migrants in weak thermal conditions. *Movement Ecology*, *11*(1), 76. https://doi.org/10.1186/s40462-023-00438-6

Spanoghe, G., Janssens, K., Klaassen, R., Schaub, T., Milotic, T., & Desmet, P. (2024). *BOP_RODENT - Rodent specialized birds of prey (Circus, Asio, Buteo) in Flanders (Belgium)* [Dataset]. Research Institute for Nature and Forest (INBO). https://doi.org/10.5281/zenodo.12567894

Spanoghe, G., Janssens, K., Nijs, G., Milotic, T., & Desmet, P. (2024). *CURLEW_VLAANDEREN - Eurasian curlews (Numenius arquata, Scolopacidae) breeding in Flanders (Belgium)* [Dataset]. Research Institute for Nature and Forest (INBO). https://doi.org/10.5281/zenodo.12587129

Stienen, E. W. M., Desmet, P., Milotic, T., Hernandez, F., Deneudt, K., Matheve, H., & Bouten, W. (2023). *HG_OOSTENDE - Herring gulls (Larus argentatus, Laridae) breeding at the southern North Sea coast (Belgium)* [Dataset]. Research Institute for Nature and Forest (INBO). https://doi.org/10.5281/zenodo.10054230

Stienen, E. W. M., Desmet, P., Milotic, T., Spanoghe, G., & Janssens, K. (2024). *MEDGULL_ANTWERPEN - Mediterranean gulls (Ichthyaetus melanocephalus, Laridae) breeding near Antwerp (Belgium)* [Dataset]. Research Institute for Nature and Forest (INBO). https://doi.org/10.5281/zenodo.12623583

Stienen, E. W. M., Mülller, W., Lens, L., Milotic, T., & Desmet, P. (2024). *LBBG_ADULT - Lesser black-backed gulls (Larus fuscus, Laridae) breeding in Belgium* [Dataset]. Research Institute for Nature and Forest (INBO). https://doi.org/10.5281/zenodo.12622252

Tøttrup, A. P., Pedersen, L., Onrubia, A., Klaassen, R. H. G., & Thorup, K. (2017). Migration of red-backed shrikes from the Iberian Peninsula: Optimal or sub-optimal detour? *Journal of Avian Biology*, *48*(1), 149–154. https://doi.org/10.1111/jav.01352

van der Kolk, H.-J., Oosterbeek, K., Jongejans, E., Frauendorf, M., Allen, A. M., Bouten, W., Desmet, P., de Kroon, H., Ens, B. J., & van de Pol, M. (2023). *O_VLIELAND - Eurasian oystercatchers (Haematopus ostralegus, Haematopodidae) breeding and wintering on Vlieland (the Netherlands)* [Dataset]. Research Institute for Nature and Forest (INBO). https://doi.org/10.5281/zenodo.10053988

van Toor, M. L., Kharitonov, S., Švažas, S., Dagys, M., Kleyheeg, E., Müskens, G., Ottosson, U., Žydelis, R., & Waldenström, J. (2021). Migration distance affects how closely Eurasian wigeons follow spring phenology during migration. *Movement Ecology*, *9*(1), 61. https://doi.org/10.1186/s40462-021-00296-0

Wikelski, M., Arriero, E., Gagliardo, A., Holland, R. A., Huttunen, M. J., Juvaste, R., Mueller, I., Tertitski, G., Thorup, K., Wild, M., Alanko, M., Bairlein, F., Cherenkov, A., Cameron, A., Flatz, R., Hannila, J., Hüppop, O., Kangasniemi, M., Kranstauber, B., … Wistbacka, R. (2015). True navigation in migrating gulls requires intact olfactory nerves. *Scientific Reports*, *5*(1), 17061. https://doi.org/10.1038/srep17061

SUPPORTING INFORMATIONS OF:

Towards a tracking of bird migratory behaviour through geological time: an isotopic and histological approach

Anaïs Duhamel[1,*], Aurore Canoville[2,3], Arnaud Vinçon-Laugier[1], Julien Joseph[4], François Fourel[4], Christophe Lécuyer[1], Romain Amiot[1,$] and Antoine Louchart[1,$]

[1] Univ Lyon, Univ Lyon 1, ENSL, CNRS, LGL-TPE, Villeurbanne, France
[2] Museum für Naturkunde, Leibniz-Institut für Evolutions- und Biodiversitätsforschung, 10115 Berlin, Germany
[3] North Carolina Museum of Natural Sciences, 27601 Raleigh NC, USA
[4] Université Claude Bernard Lyon 1, LEHNA UMR 5023, CNRS, ENTPE, F-69622 Villeurbanne, France
[*] Corresponding author, anais.duhamel@ens-lyon.fr
[$] Co-senior authors

CONTENT

APPENDIX A: Preliminary tests protocols to control for potential biases on bones isotopic composition.

FIGURE S1: Influence of heterothermy (B) and sodium perborate treatment (C) on bones' δ18Op.

APPENDIX B: Diagnostic criteria to identify and quantify bone tissues on thin sections.

FIGURE S2: Natural (A, B, D) and polarized light (C, E, F) images showing bone tissues in extant (A-E) and fossil (F) adult birds, illustrating the diagnostic criteria developed in Appendix A.

FIGURE S3: Map depicting year-round living location of sedentary individuals, drawn from the revised 2023 eBird Basic Dataset. Individuals are color-coded by species.

FIGURE S4: Map depicting one year of migratory routes for each individual, derived from data available in the Movebank.org repository (see Data Source section). Individuals are color-coded by species.

FIGURE S5: Comparison of fractionation equations linking drinking water $\delta^{18}O_w$ estimates to bone phosphate $\delta^{18}O_p$ measurements in birds, using reduced major axis (RMA) regression.

FIGURE S6: Distribution of Spearman's ρ coefficients obtained for correlations (p-value<0.05) between f_{LBT} and $\delta^{18}O_{p,\ bulk}$ values in migratory, temperate and tropical sedentary birds.

FIGURE S7: Distribution of Spearman's ρ coefficients obtained for significant correlations (p-value<0.05) between f_{LBT} and $\delta^{18}O_{p,\ bulk}$ values in migratory, temperate and tropical sedentary birds.

FIGURE S8: Theoretical specificity of the test identifying migratory behaviour ("positive" outcome) based on significantly positive correlations between f_{LBT} and $\delta^{18}O_{p,\ bulk}$ (i.e., Spearman's ρ>0 and p-value<0.05).

FIGURE S9: Theoretical sensitivity of the test identifying migratory behaviour ("positive" outcome) based on significantly positive correlations between f_{LBT} and $\delta^{18}O_{p,\ bulk}$ (i.e., Spearman's ρ>0 and p-value<0.05).

FIGURE S10: Theoretical specificity of the test identifying sedentary behaviour ("positive" outcome) based on significantly negative correlations between f_{LBT} and $\delta^{18}O_{p,\ bulk}$ (i.e., Spearman's ρ<0 and p-value<0.05).

FIGURE S11: Theoretical sensitivity of the test identifying sedentary behaviour ("positive" outcome) based on significantly negative correlations between f_{LBT} and $\delta^{18}O_{p,\ bulk}$ (i.e., Spearman's ρ<0 and p-value<0.05).

FIGURE S12: Death locations of migratory individuals from the application case, and known breeding and non-breeding areas of their species (modified after eBird maps; Sullivan et al., 2009).

APPENDIX REFERENCES

APPENDIX A. Preliminary tests protocols to control for potential biases on bones isotopic composition

A.1 Test the influence of sodium perborate treatment on bone isotopic value

A sodium perborate treatment was historically performed to clean the skeletal specimens of the Collections de l'Université de Lyon 1 from their tendinous and cartilaginous parts. We therefore controlled the influence of such chemical – which contains oxygen – on the oxygen isotope ratios of bone tissues. We compared the oxygen isotope ratio of two subsamples deriving from the same bone sample of a Great cormorant: one of it treated using sodium perborate, the other remaining untreated. The sodium perborate treatment consisted in boiling the bone sample several hours in a 2 $g.L^{-1}$ boiling sodium perborate solution. This treatment appears to have no significant effect on the oxygen isotope ratio of a test individual's bones (Fig S1).

A.2 Skeleton isotopic cartography to test potential heterothermies

Oxygen isotopic fractionation is known to be temperature-dependent. Given that birds are endotherms, and that some bones are surrounded by more soft tissues than others, fleshy body-parts are supposed to be controlled by the constant body temperature around 40°C in birds, while skinnier body parts temperature is supposed to be closer to the air temperature. We therefore carried out an isotopic mapping of the skeleton of a juvenile bird to test whether potential heterothermies at the skeletal scale affect the oxygen isotopic fractionation during bone mineralisation. The control specimen was chosen juvenile to avoid the bias associated with bone remodeling, which can vary between bones. This test was run on 6 different post-cranial bones of a juvenile extant chicken (Fig S1, A). As we found no significant difference in oxygen isotope fractionation between the bones of the chicks belonging to more or less fleshy body parts (Fig S1), isotopic fractionation was considered homogeneous at the individual level, regardless of potential heterothermies within the body.

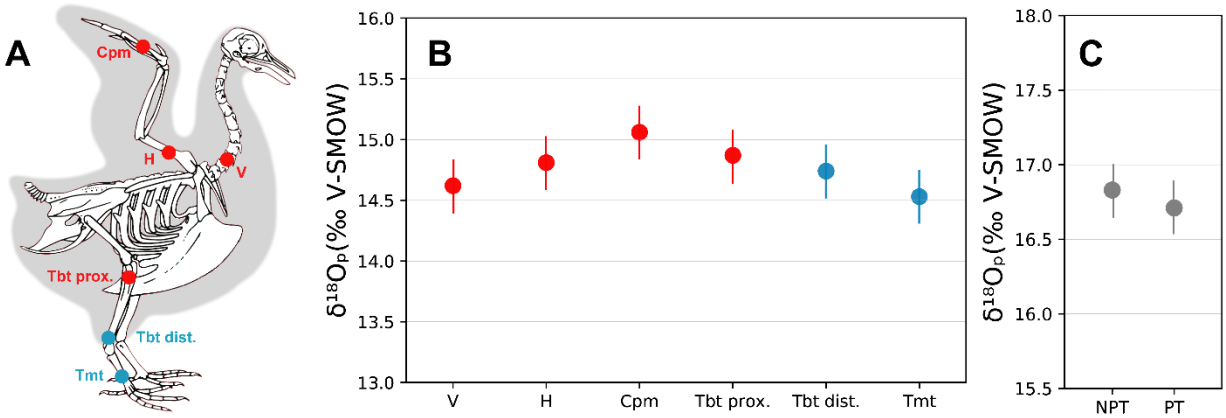

FIGURE S1: Influence of heterothermy (B) and sodium perborate treatment (C) on bones' $\delta^{18}O_p$. A: shows the fleshiness of the chicken body parts surrounding the bone tested for the heterothermy test, red points for fleshy parts and blue point for relatively less fleshy parts on both A and B. Abbreviations: V, vertebrae; H, humerus; Cpm, carpometacarpus; Tbt prox., proximal tibiotarsus; Tbt dist., distal tibiotarsus; Tmt, tarsometatarsus; NPT, no perborate treatment; PT, perborate treatment. Error bars are the mean analytical error for all chemistries (±0.22 ‰).

APPENDIX B. Diagnostic criteria to identify and quantify histological features on thin sections

Secondary osteons can be distinguished from primary osteons based on the several characteristics, as follows:

(i) They are surrounded by a cement line (Fig. S2, b, d), which is the result of their particular formation process. Indeed, the cement line results from the local resorption of bone by osteoclasts in the cortex, and the subsequent centripetal deposition of secondary bone by osteoblast cells. The cement line is scalloped, delimitates each individual secondary osteon, and marks the interface between tissues deposited at different time intervals. By definition, primary osteons are not surrounded by a cement line.

(ii) This continuous process of resorption-redeposition, characteristic of bone remodeling, can also have for consequence a possible overlap between different secondary osteons generations as shown in Fig. S2, f, and an overlap on underlying primary bone tissues.

(iii) Moreover, remodeling and the associated formation of secondary osteons are usually initiated in the peri-medullary, deep cortical region and extend progressively towards the periosteal surface throughout the life of an individual. In birds, secondary osteons are thus preferentially concentrated in the deep and mid cortex, whereas primary osteons found in the primary fibrolamellar tissue form more homogeneously throughout the cortex.

(iv) Another characteristic feature is that in birds, in general, secondary osteons are larger in diameter than primary osteons and also that their shape is less homogeneous.

(v) Finally, secondary osteons are formed of an avascular parallel-fibered or lamellar bone matrix and thus have a different texture than the surrounding fibrolamellar bone under both natural and polarized light (Fig. S2, a, c, e, f).

Note that Maltese crosses, which are artefacts visible on osteons in polarized light (Fig. S2, e), are often considered as a diagnostic criterion for secondary osteons, but were here occasionally observed on primary osteons.

Most of the primary periosteal cortex is formed of a well-vascularized fibrolamellar bone (woven bone matrix associated to primary osteons) in birds. Towards the end of growth, there is also formation of an inner circumferential layer (ICL) and outer circumferential layer (OCL). OCL is primary bone in most cases, but can also be secondary bone made of poorly vascularized to avascular parallel-fibered bone tissue, the ICL is always made of avascular endosteal lamellar bone. The deposition of the ICL marks the end of the medullary cavity expansion. The deposition of the OCL marks the attainment of skeletal maturity. The OCL and ICL are easily distinguishable from other bone features (such as secondary osteons) and appear clearly birefringent under polarized light (linked to the orientation of collagen fibers and hydroxyapatite crystals, Chinsamy, 2005, Fig. S2, c, e, f). In rare cases, secondary osteons can form before the end of the chick's development (so before the OCL formation) to repair fractures, micro-damages, or because the chick went through an unusual stress-inducing event. This early remodeling event can be recognized by secondary osteons being cross-cut by the ICL (Fig. S2, f), but is hard to quantify because of the possible overlying of several generations of secondary osteons. It is therefore a potential source of error on proportion determination.

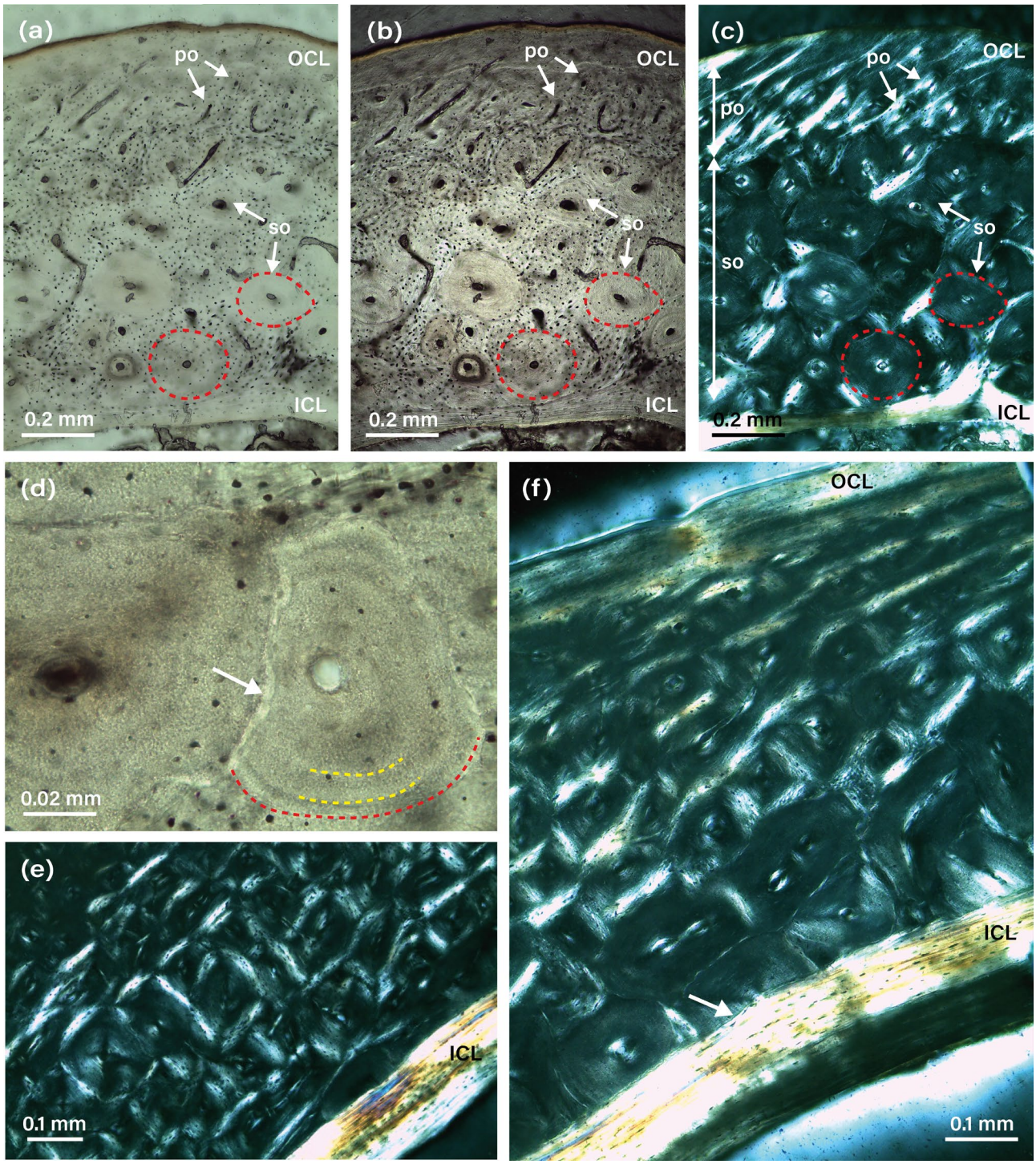

FIGURE S2: Natural (a, b, d) and polarized light (c, e, f) images showing bone tissues in extant adult birds, illustrating the diagnostic criteria developed in Appendix A. (a), (b) and (c) show the same region of a White Stork (*Ciconia ciconia*) tibiotarsus under different lights, and a zoom on secondary osteons. (d) shows the cement line delimiting the osteons (red dotted line), lamellae (yellow dotted lines), and an overlapping relationship between osteons (white arrow). Note that limiting the transmitted light amount with the microscope condenser makes secondary osteons cement line more visible (b, d), and that primary fibrolamellar bone between primary (po) and secondary osteons (so) appears highly birefringent in polarizing light. Inner (ICL) and outer circumferential layers (OCL) appear also very bright in polarizing light. (e) *Grus grus* tibiotarsus detail showing maltese crosses within secondary osteons. (f) *Grus grus* tibiotarsus showing secondary osteons cut by the ICL, evidence that this bone remodelling took place when the bird was juvenile. Conventionally, all the images are oriented with the medullary cavity on the bottom.

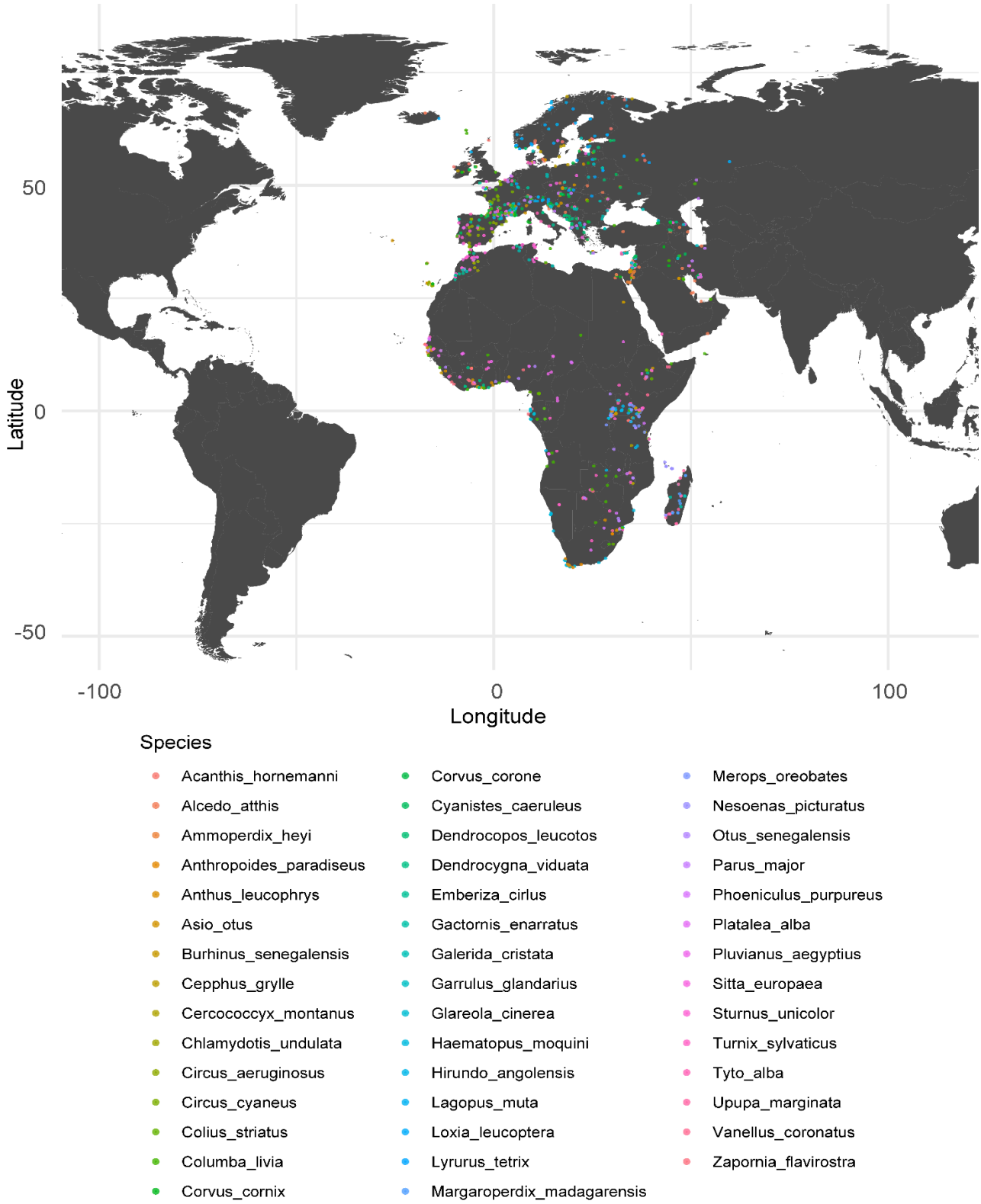

FIGURE S3: Map depicting year-round living location of sedentary individuals, drawn from the revised 2023 eBird Basic Dataset. Individuals are color-coded by species.

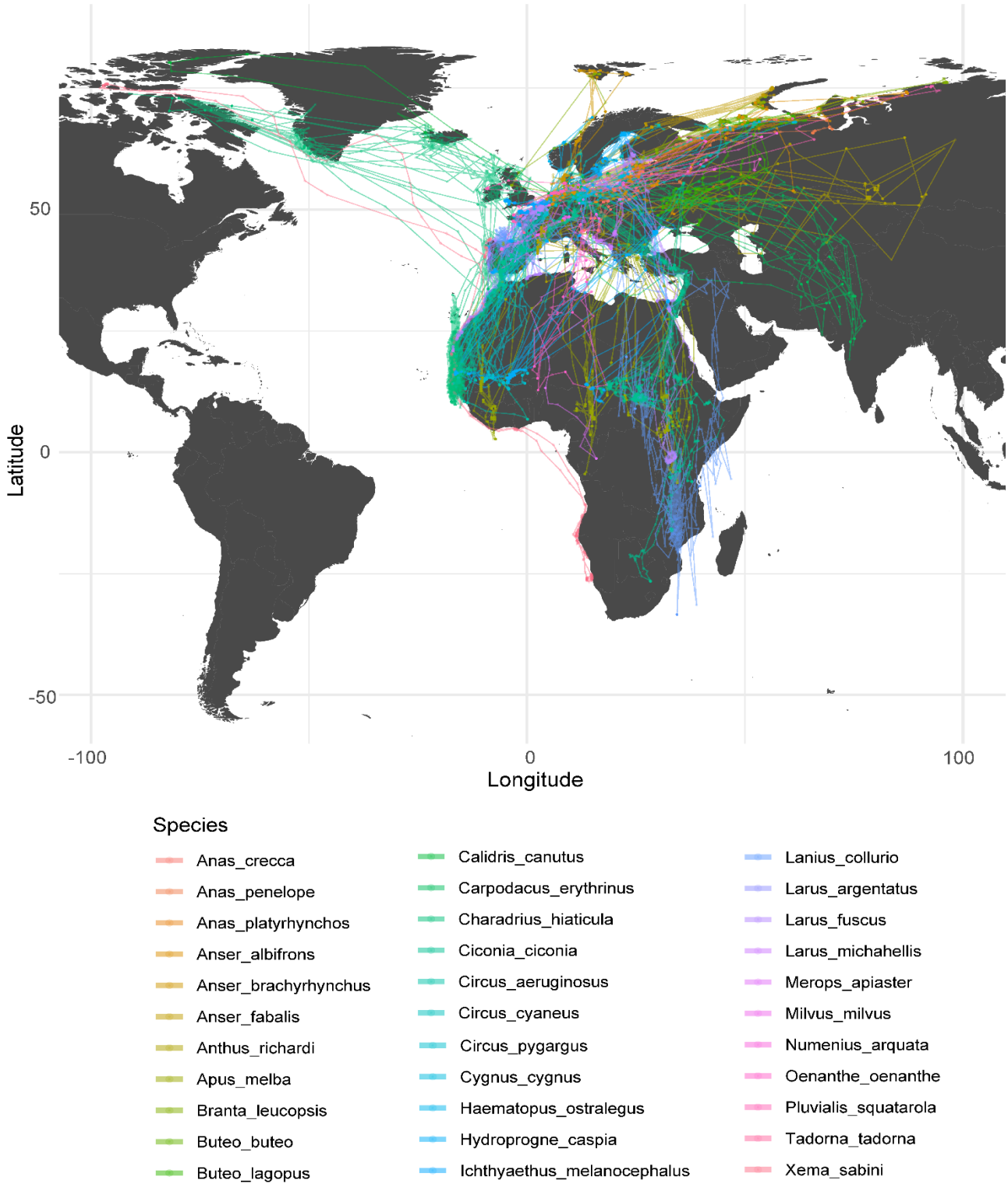

FIGURE S4: Map depicting one year of migratory routes for each individual, derived from data available in the Movebank.org repository (see Data Source section and Table S1). Individuals are color-coded by species.

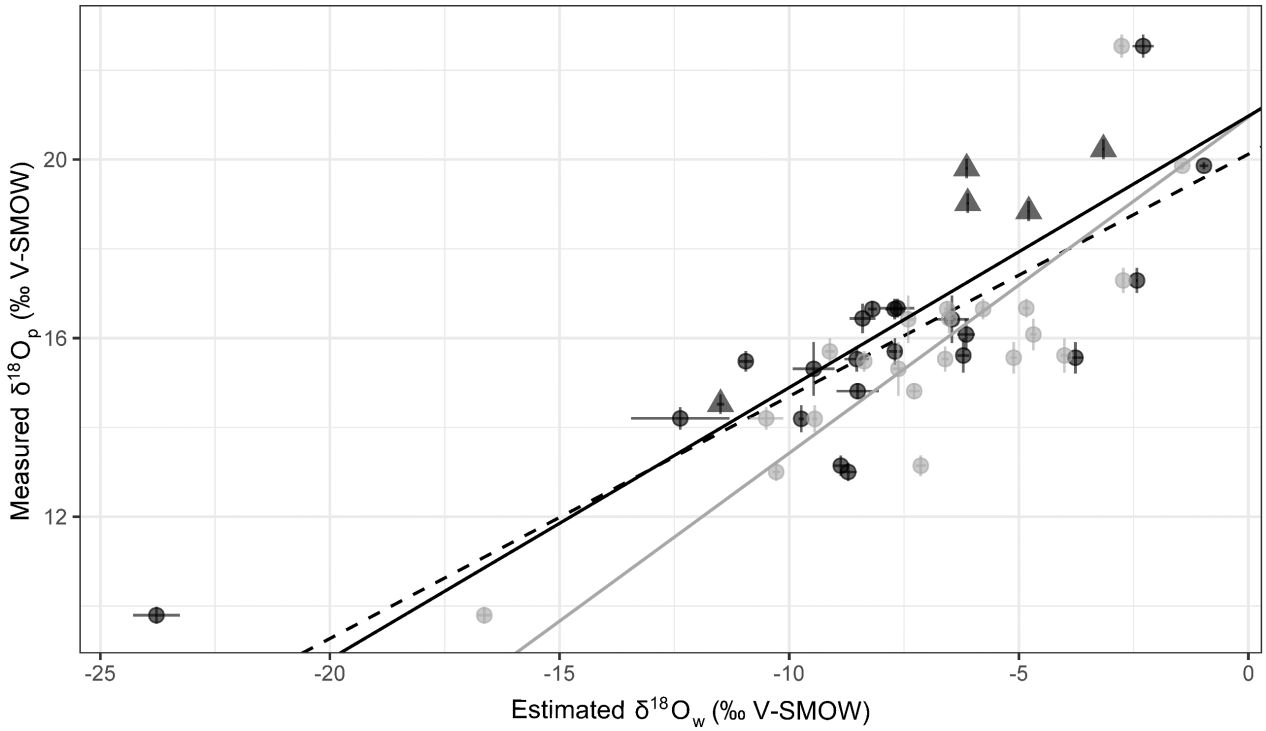

Amiot et al. (2017) $\delta^{18}O_p$ measurements on juvenile broiler chicken, associated with the local mean annual $\delta^{18}O_w$ estimates

Amiot et al. (2017) $\delta^{18}O_p$ measurements on juvenile broiler chicken, associated with the mean annual $\delta^{18}O_w$ estimates of the individual's lifetime (modelled as a 30-day period).

Present paper $\delta^{18}O_p$ measurements from the ulnar midshaft of wild juvenile and sedentary birds, associated with the mean annual $\delta^{18}O_w$ estimates for the individual's lifetime (modelled as a 30-day period).

RMA regression on ● : $\delta^{18}O_p = 0.75\ \delta^{18}O_w + 20.95$ (eqn 2)
$R^2 = 0.699$; p-value = 2.35e-06 ; Standard error on $\delta^{18}O_p$ residuals = 1.396 ‰

RMA regression on ● : $\delta^{18}O_p = 0.54\ \delta^{18}O_w + 20.12$ (eqn 2b)
$R^2 = 0.659$; p-value = 8.00e-06 ; Standard error on $\delta^{18}O_p$ residuals = 1.497 ‰

RMA regression on ● and ▲ : $\delta^{18}O_p = 0.61\ \delta^{18}O_w + 20.97$ (eqn 3)
$R^2 = 0.647$; p-value = 7.32e-07 ; Standard error on $\delta^{18}O_p$ residuals = 1.626 ‰

FIGURE S5: Comparison of fractionation equations linking drinking water $\delta^{18}O_w$ estimates to bone phosphate $\delta^{18}O_p$ measurements in birds, using reduced major axis (RAM) regression. The fit was performed either on the raw $\delta^{18}O_p$ and $\delta^{18}O_w$ data from Amiot et al. (2017) (equation 2 in the main text), on the $\delta^{18}O_p$ from Amiot et al. (2017) against revised $\delta^{18}O_w$ estimates (equation 2b), or on the same dataset extended with control data from the present study (juvenile and sedentary birds) (equation 3 in the main text).

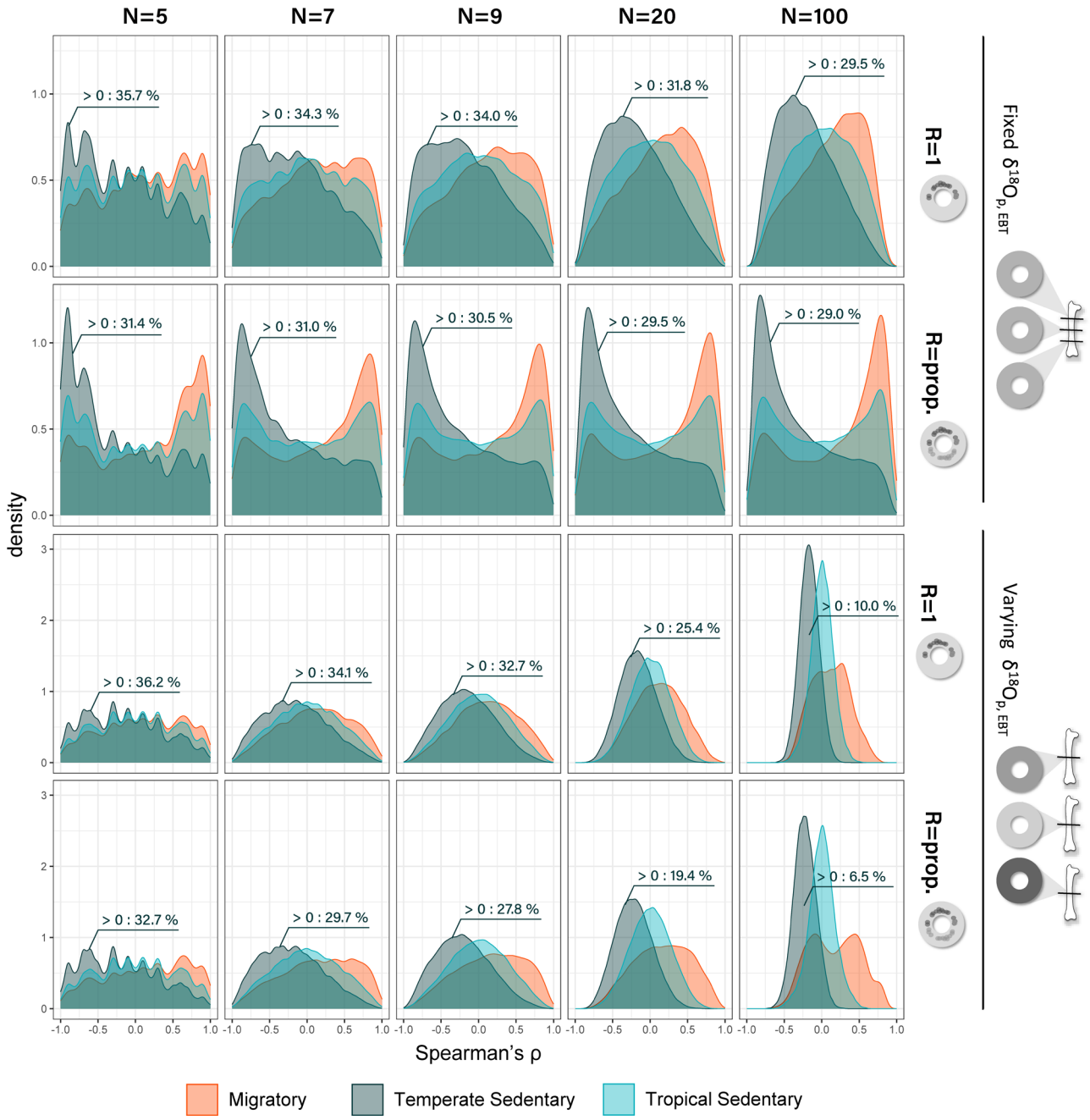

FIGURE S6: Distribution of Spearman's ρ coefficients obtained for correlations (p-value<0.05) between f_{LBT} and $\delta^{18}O_{p,\ bulk}$ values in migratory, temperate and tropical sedentary birds. Correlation was tested on samplings of varying sizes (*N*=5, 7, 9, 20 or 100), varying number of bone remodelling events per sample (*R*=1 or *R*=prop.), and sampling conducted either within a single individual (fixed $\delta^{18}O_{p,\ EBT}$ values) or within individuals of the same populations (varying $\delta^{18}O_{p,\ EBT}$ values). *N*-sized sampling was repeated 100 times per population.

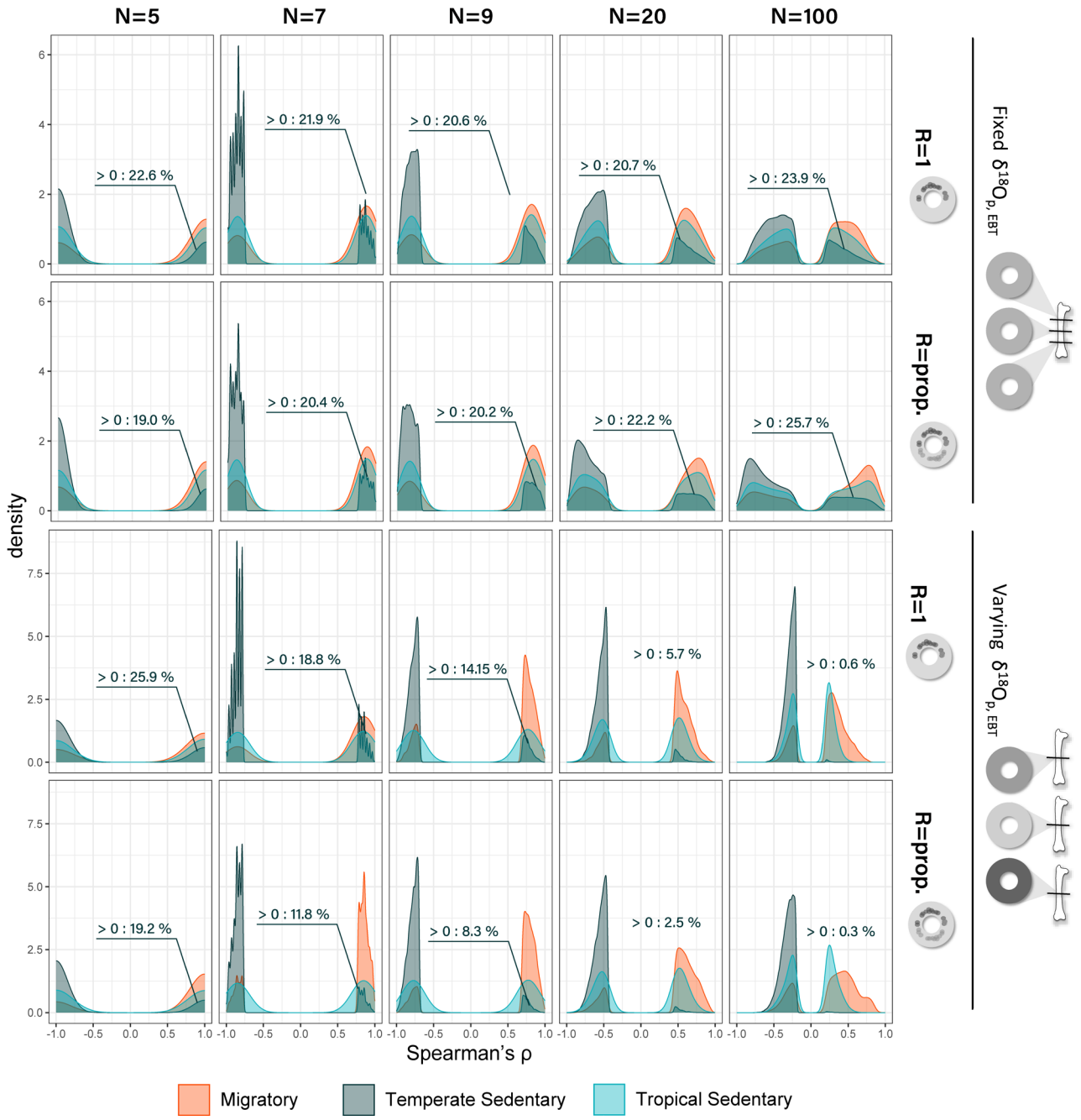

FIGURE S7: Distribution of Spearman's ρ coefficients obtained for significant correlations (p-value<0.05) between f_{LBT} and $\delta^{18}O_{p,\ bulk}$ values in migratory, temperate and tropical sedentary birds. Correlation was tested on samplings of varying sizes (*N*=5, 7, 9, 20 or 100), varying number of bone remodelling events per sample (*R*=1 or *R*=prop.), and sampling conducted either within a single individual (fixed $\delta^{18}O_{p,\ EBT}$ values) or within individuals of the same populations (varying $\delta^{18}O_{p,\ EBT}$ values). *N*-sized sampling was repeated 100 times per population.

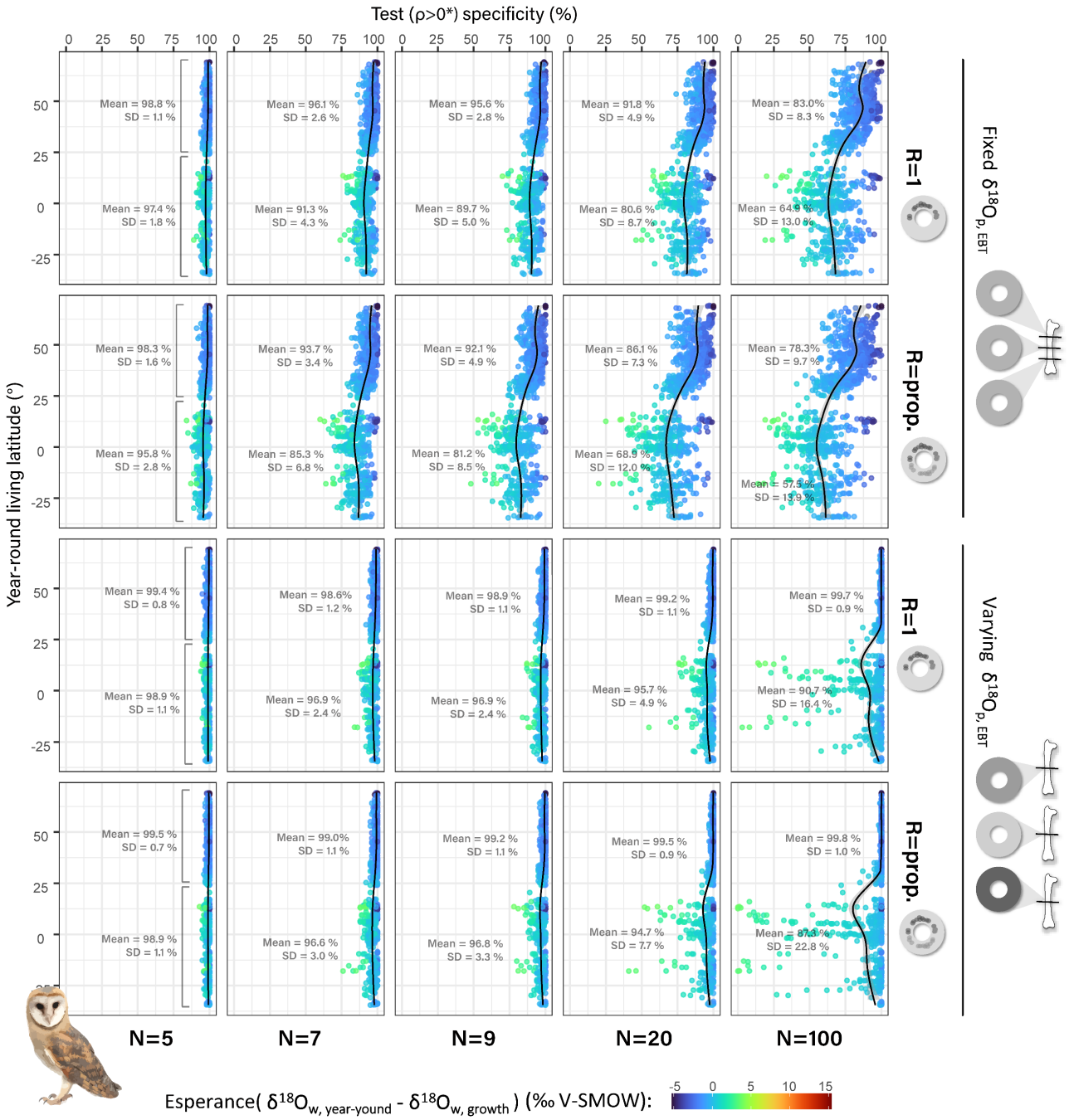

FIGURE S8: Theoretical specificity of the test identifying migratory behaviour ("positive" outcome) based on significantly positive correlations between f_{LBT} and $\delta^{18}O_{p,\ bulk}$ (i.e., Spearman's $\rho>0$ and p-value<0.05). This decision rule was applied to samplings of varying sizes (N=5, 7, 9, 20 or 100), varying number of bone remodelling events per sample (R=1 or R=prop.), and with the N samples coming either from a single individual (fixed $\delta^{18}O_{p,\ EBT}$ values) or from individuals of the same population (varying $\delta^{18}O_{p,\ EBT}$ values). N-sized sampling was repeated 100 times per population, allowing calculation of population-specific specificities (1 – proportion of false positives). Specificities were plotted against the living latitude of sedentary birds, and coloured according to the population's mean difference between $\delta^{18}O$ values of year-round and growth-period rainwater.

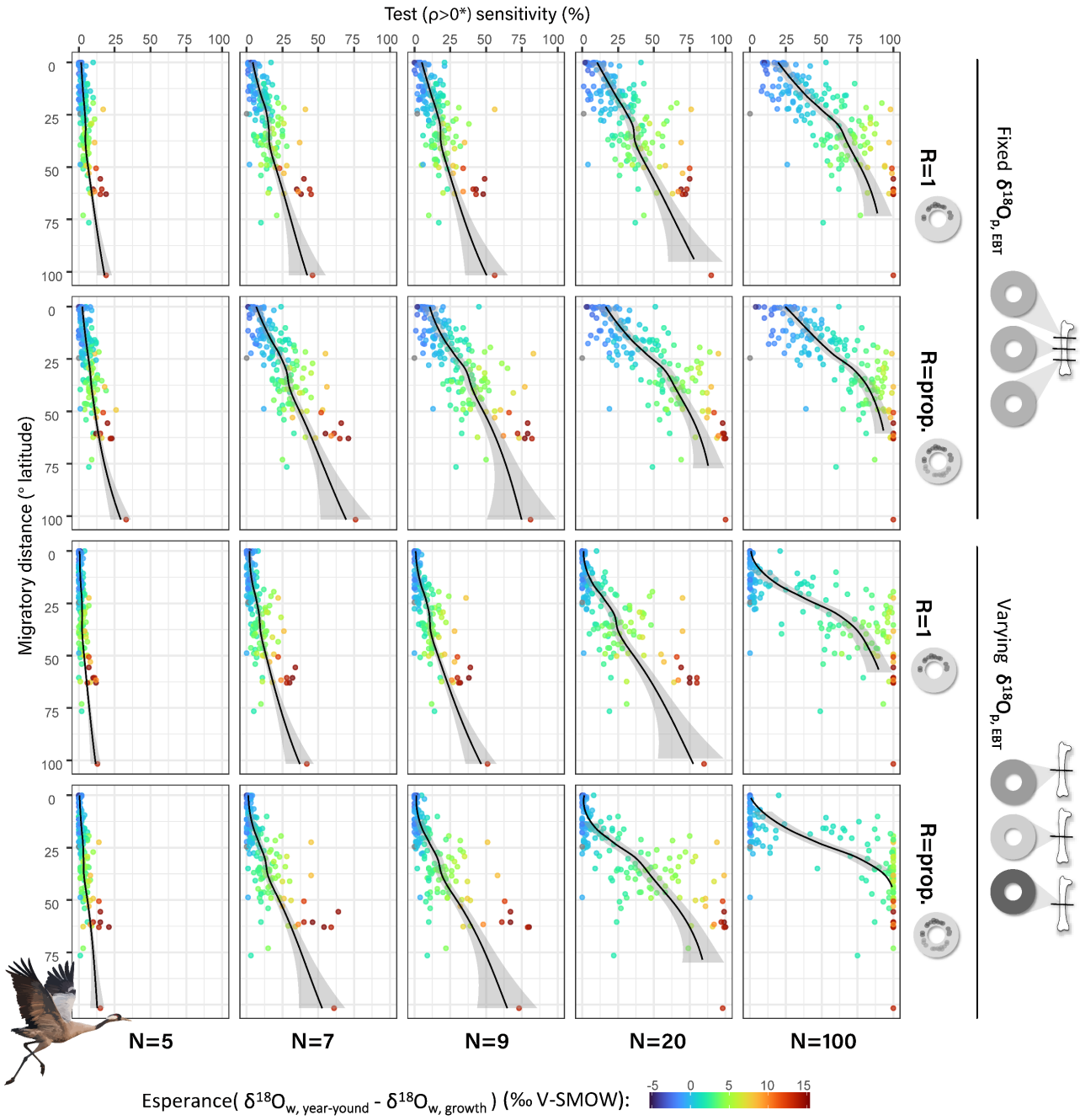

FIGURE S9: Theoretical sensitivity of the test identifying migratory behaviour ("positive" outcome) based on significantly positive correlations between f_{LBT} and $\delta^{18}O_{p,\ bulk}$ (i.e., Spearman's $\rho>0$ and p-value<0.05). This decision rule was applied to samplings of varying sizes (N=5, 7, 9, 20 or 100), varying number of bone remodelling events per sample (R=1 or R=prop.), and with the N samples coming either from a single individual (fixed $\delta^{18}O_{p,\ EBT}$ values) or from individuals of the same population (varying $\delta^{18}O_{p,\ EBT}$ values). N-sized sampling was repeated 100 times per population, allowing calculation of population-specific sensitivity (proportion of true positives). Sensitivity were plotted against the living latitude of sedentary birds, and coloured according to the population's mean difference between $\delta^{18}O$ values of year-round and growth-period rainwater.

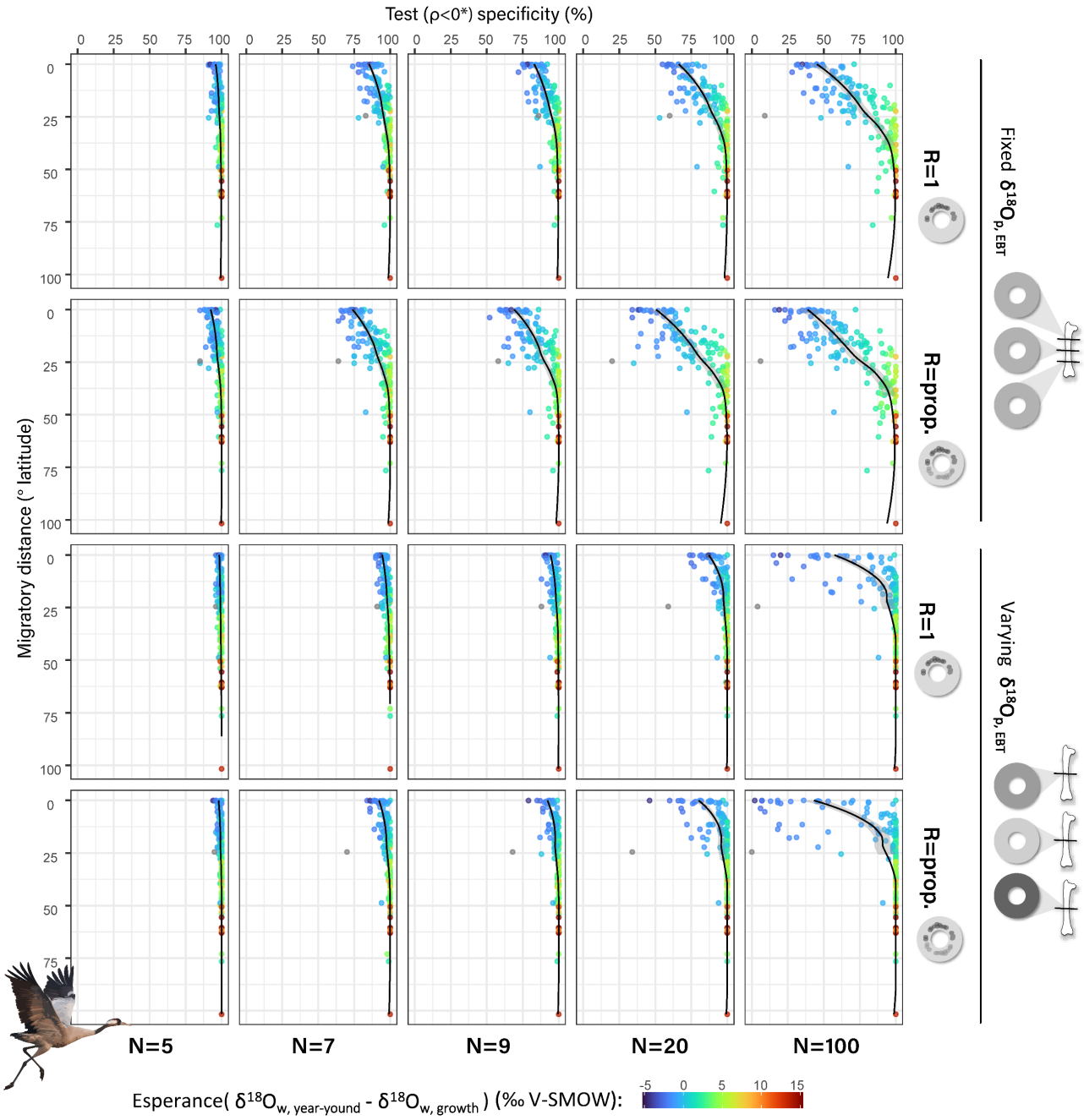

FIGURE S10: Theoretical specificity of the test identifying sedentary behaviour ("positive" outcome) based on significantly negative correlations between f_{LBT} and $\delta^{18}O_{p,\ bulk}$ (i.e., Spearman's $\rho<0$ and p-value<0.05). This decision rule was applied to samplings of varying sizes (N=5, 7, 9, 20 or 100), varying number of bone remodelling events per sample (R=1 or R=prop.), and with the N samples coming either from a single individual (fixed $\delta^{18}O_{p,\ EBT}$ values) or from individuals of the same population (varying $\delta^{18}O_{p,\ EBT}$ values). N-sized sampling was repeated 100 times per population, allowing calculation of population-specific specificities (1 – proportion of false positives). Specificities were plotted against the living latitude of sedentary birds, and coloured according to the population's mean difference between $\delta^{18}O$ values of year-round and growth-period rainwater.

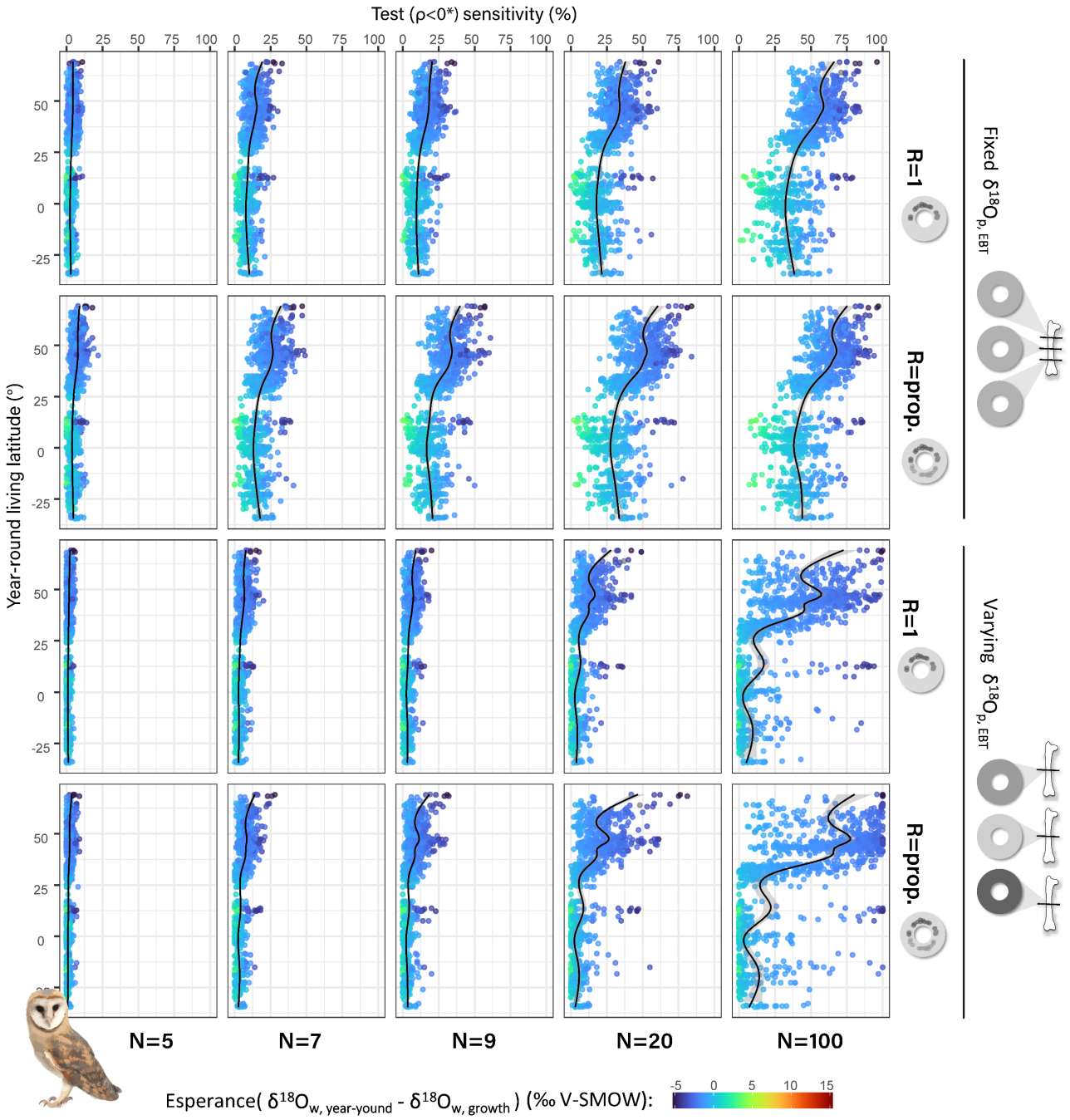

FIGURE S11: Theoretical sensitivity of the test identifying sedentary behaviour ("positive" outcome) based on significantly negative correlations between f_{LBT} and $\delta^{18}O_{p,\ bulk}$ (i.e., Spearman's $\rho<0$ and p-value<0.05). This decision rule was applied to samplings of varying sizes (N=5, 7, 9, 20 or 100), varying number of bone remodelling events per sample (R=1 or R=prop.), and with the N samples coming either from a single individual (fixed $\delta^{18}O_{p,\ EBT}$ values) or from individuals of the same population (varying $\delta^{18}O_{p,\ EBT}$ values). N-sized sampling was repeated 100 times per population, allowing calculation of population-specific sensitivity (proportion of true positives). Sensitivities were plotted against the living latitude of sedentary birds, and coloured according to the population's mean difference between $\delta^{18}O$ values of year-round and growth-period rainwater.

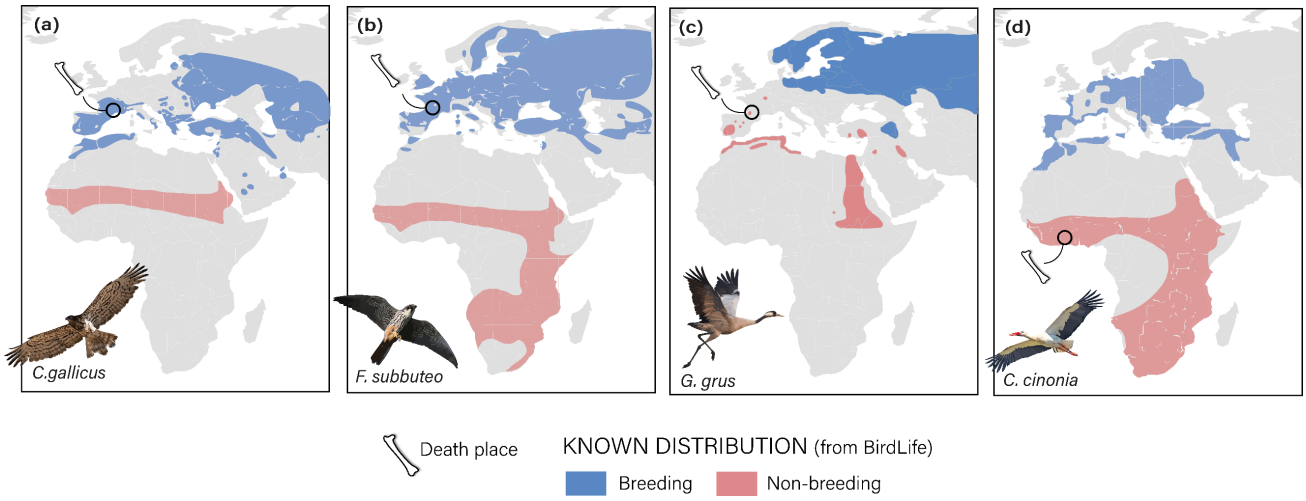

FIGURE S12: Death locations of migratory individuals from the application case, and known breeding and non-breeding areas of their species (modified after eBird data maps; Sullivan et al., 2009).

APPENDIX REFERENCES

Amiot, R., Angst, D., Legendre, S., Buffetaut, E., Fourel, F., Adolfssen, J., André, A., Bojar, A. V., Canoville, A., Barral, A., Goedert, J., Halas, S., Kusuhashi, N., Pestchevitskaya, E., Rey, K., Royer, A., Saraiva, A. Á. F., Savary-Sismondini, B., Siméon, J.-L., … Lécuyer, C. (2017). Oxygen isotope fractionation between bird bone phosphate and drinking water. *The Science of Nature*, *104*(5–6), 47. https://doi.org/10.1007/s00114-017-1468-2

Chinsamy-Turan, A. (2005). *The Microstructure of Dinosaur Bone | Hopkins Press*. https://press.jhu.edu/books/title/3496/microstructure-dinosaur-bone

Sullivan, B. L., Wood, C. L., Iliff, M. J., Bonney, R. E., Fink, D., & Kelling, S. (2009). eBird: A citizen-based bird observation network in the biological sciences. *Biological Conservation*, *142*(10), 2282–2292. https://doi.org/10.1016/j.biocon.2009.05.006